Inverse Problems for the Dynamic Euler-Bernoulli Beam Equation: Theory and Applications

Alemdar Hasanov Hasanoglu

Department of Mathematics, Kocaeli University, Turkey

Joint Seminar on Inverse Problems
CNRS (UMR 7641), Centre de Mathématiques Appliquées, École Polytechnique, Paris

September 17, 2019

SUPPORTS

1. The research has been supported by

SUPPORTS

1. The research has been supported by
2. CMAP -Centre de Mathématiques Appliquées, Ecole Polytechnique, France

SUPPORTS

1. The research has been supported by
2. CMAP -Centre de Mathématiques Appliquées, Ecole Polytechnique, France
3. The Japan Society for the Promotion of Science (JSPS), through the International Program FY2018, 2018

CONTENT

1. Typical/basic inverse problems based on available/feasible boundary measured data and real (physical and engineering) requirements

CONTENT

1. Typical/basic inverse problems based on available/feasible boundary measured data and real (physical and engineering) requirements
2. Brief history and literature review

CONTENT

1. Typical/basic inverse problems based on available/feasible boundary measured data and real (physical and engineering) requirements
2. Brief history and literature review
3. Main principles of the proposed approach

CONTENT

1. Typical/basic inverse problems based on available/feasible boundary measured data and real (physical and engineering) requirements
2. Brief history and literature review
3. Main principles of the proposed approach
4. Compactness of the input-output operators. Ill-posedness

CONTENT

1. Typical/basic inverse problems based on available/feasible boundary measured data and real (physical and engineering) requirements
2. Brief history and literature review
3. Main principles of the proposed approach
4. Compactness of the input-output operators. Ill-posedness
5. Existence and uniqueness of the solutions to the inverse problems

CONTENT

1. Typical/basic inverse problems based on available/feasible boundary measured data and real (physical and engineering) requirements
2. Brief history and literature review
3. Main principles of the proposed approach
4. Compactness of the input-output operators. Ill-posedness
5. Existence and uniqueness of the solutions to the inverse problems
6. Adjoint method: Fréchet differentiability of the Tikhonov functional

CONTENT

1. Typical/basic inverse problems based on available/feasible boundary measured data and real (physical and engineering) requirements
2. Brief history and literature review
3. Main principles of the proposed approach
4. Compactness of the input-output operators. Ill-posedness
5. Existence and uniqueness of the solutions to the inverse problems
6. Adjoint method: Fréchet differentiability of the Tikhonov functional
7. Lipschitz continuity of Fréchet gradient implies the monotonicity of gradient algorithm

CONTENT

1. Typical/basic inverse problems based on available/feasible boundary measured data and real (physical and engineering) requirements
2. Brief history and literature review
3. Main principles of the proposed approach
4. Compactness of the input-output operators. Ill-posedness
5. Existence and uniqueness of the solutions to the inverse problems
6. Adjoint method: Fréchet differentiability of the Tikhonov functional
7. Lipschitz continuity of Fréchet gradient implies the monotonicity of gradient algorithm
8. Numerical algorithms based on Hermitian FEM and CG-algorithm

CONTENT

1. Typical/basic inverse problems based on available/feasible boundary measured data and real (physical and engineering) requirements
2. Brief history and literature review
3. Main principles of the proposed approach
4. Compactness of the input-output operators. Ill-posedness
5. Existence and uniqueness of the solutions to the inverse problems
6. Adjoint method: Fréchet differentiability of the Tikhonov functional
7. Lipschitz continuity of Fréchet gradient implies the monotonicity of gradient algorithm
8. Numerical algorithms based on Hermitian FEM and CG-algorithm
9. Results of numerical experiments

CONTENT

1. Typical/basic inverse problems based on available/feasible boundary measured data and real (physical and engineering) requirements
2. Brief history and literature review
3. Main principles of the proposed approach
4. Compactness of the input-output operators. Ill-posedness
5. Existence and uniqueness of the solutions to the inverse problems
6. Adjoint method: Fréchet differentiability of the Tikhonov functional
7. Lipschitz continuity of Fréchet gradient implies the monotonicity of gradient algorithm
8. Numerical algorithms based on Hermitian FEM and CG-algorithm
9. Results of numerical experiments
10. Unsolved Problems

1.1a. Inverse Temporal Source Problems (ITSP)

Identification of a temporal load in a cantilever beam from measured boundary bending moment

Consider the *inverse problem of identifying the unknown temporal load* $G(t)$

1. in a system governed initial-boundary value problem

$$\begin{cases} \rho(x)u_{tt} + \mu(x)u_t + (r(x)u_{xx})_{xx} = F(x)G(t), \text{ in } \Omega_T := (0,\ell)\times(0,T), \\ u(x,0) = 0,\ \ u_t(x,0) = 0, \quad x\in(0,\ell), \\ u(0,t) = u_x(0,t) = 0,\ \ r(\ell)u_{xx}(\ell,t) = (r(\ell)u_{xx}(\ell,t))_x = 0,\ \ t\in[0,T], \end{cases} \tag{1}$$

1.1a. Inverse Temporal Source Problems (ITSP)

Identification of a temporal load in a cantilever beam from measured boundary bending moment

Consider the *inverse problem of identifying the unknown temporal load* $G(t)$

1. in a system governed initial-boundary value problem

$$\begin{cases} \rho(x)u_{tt} + \mu(x)u_t + (r(x)u_{xx})_{xx} = F(x)G(t), \text{ in } \Omega_T := (0,\ell) \times (0,T), \\ u(x,0) = 0, \;\; u_t(x,0) = 0, \quad x \in (0,\ell), \\ u(0,t) = u_x(0,t) = 0, \;\; r(\ell)u_{xx}(\ell,t) = (r(\ell)u_{xx}(\ell,t))_x = 0, \;\; t \in [0,T], \end{cases} \tag{1}$$

2. from the measured bending moment $\mathcal{M}(t)$ at the left boundary of a beam:

$$\mathcal{M}(t) := -r(0)u_{xx}(0,t), \quad t \in [0,T]. \tag{2}$$

1.1a. Inverse Temporal Source Problems (ITSP)

Identification of a temporal load in a cantilever beam from measured boundary bending moment

Consider the *inverse problem of identifying the unknown temporal load* $G(t)$

1. in a system governed initial-boundary value problem

$$\begin{cases} \rho(x)u_{tt} + \mu(x)u_t + (r(x)u_{xx})_{xx} = F(x)G(t), \text{ in } \Omega_T := (0,\ell)\times(0,T), \\ u(x,0) = 0,\ \ u_t(x,0) = 0, \quad x \in (0,\ell), \\ u(0,t) = u_x(0,t) = 0,\ \ r(\ell)u_{xx}(\ell,t) = (r(\ell)u_{xx}(\ell,t))_x = 0,\ \ t \in [0,T], \end{cases} \tag{1}$$

2. from the measured bending moment $\mathcal{M}(t)$ at the left boundary of a beam:

$$\mathcal{M}(t) := -r(0)u_{xx}(0,t), \quad t \in [0,T]. \tag{2}$$

3. Here and below, $r(x) = EI(x)$, while $E > 0$ is the *elasticity modulus*, $I(x) > 0$ is the *moment of inertia of the cross-section*, $\rho(x) > 0$ is the *mass density* of the beam, $\mu(x) > 0$ is the *damping coefficient*. Without loss of generality, the initial data in (1) are assumed to be zero.

1.1b. Inverse Temporal Source Problems: Applications Overview

1. Cantilevers find extensive applications in modelling rotor blades and airplane wings

1.1b. Inverse Temporal Source Problems: Applications Overview

1. Cantilevers find extensive applications in modelling rotor blades and airplane wings
2. **Important references**: Airplane wings and helicopter rotor blade

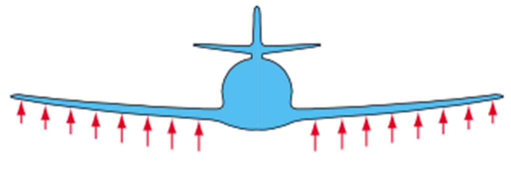

1.1b. Inverse Temporal Source Problems: Applications Overview

1. Cantilevers find extensive applications in modelling rotor blades and airplane wings
2. **Important references**: Airplane wings and helicopter rotor blade

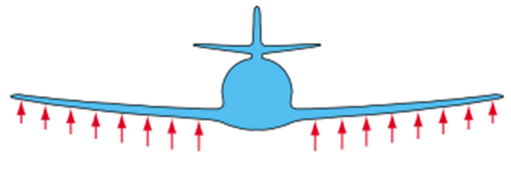

3. F.G. Polanco, Determining Beam Bending Distribution Using Dynamic Information, Report DSTO–RR–0226, *Defence Science & Technology Organization (DSTO)*, Australia, 2002

1.1b. Inverse Temporal Source Problems: Applications Overview

1. Cantilevers find extensive applications in modelling rotor blades and airplane wings
2. **Important references**: Airplane wings and helicopter rotor blade

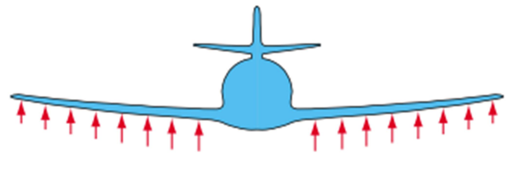

3. F.G. Polanco, Determining Beam Bending Distribution Using Dynamic Information, Report DSTO–RR–0226, *Defence Science & Technology Organization (DSTO)*, Australia, 2002
4. K.G. Vinod, S. Gopalakrishnan and R. Ganguli, Free vibration and wave propagation analysis of uniform and tapered rotating beams using spectrally formulated finite elements, *International Journal of Solids and Structures*, **44**(2007) 5875–5893.

1.1c. Inverse Temporal Source Problems: Geometry of the ITSP

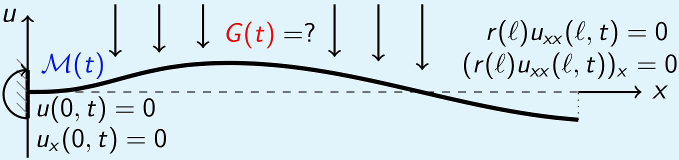

For a cantilevered beam, the boundary conditions are:

1. The Dirichler boundary conditions ("clamped end") $u(0,t) = u_x(0,t) = 0,\ t \in [0,T]$ say that the base of the beam (at the wall) does not experience any deflection and the beam at the wall is horizontal, so that the derivative of the deflection function is zero at $x = 0$.

1.1c. Inverse Temporal Source Problems: Geometry of the ITSP

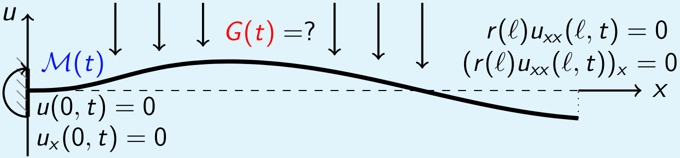

For a cantilevered beam, the boundary conditions are:

1. The Dirichler boundary conditions ("clamped end") $u(0, t) = u_x(0, t) = 0$, $t \in [0, T]$ say that the base of the beam (at the wall) does not experience any deflection and the beam at the wall is horizontal, so that the derivative of the deflection function is zero at $x = 0$.
2. The Neumann boundary conditions ("free end") $r(l)u_{xx}(l, t) = (r(l)u_{xx}(l, t))_x = 0$, $t \in [0, T]$ say that there is no bending moment and shearing force acting at the free end of the beam.

1.1d. ITSP: Other Physical Models

There exist other physical models with the following Dirichlet type measured outputs

Consider the following two basic inverse temporal source problems.

1. Find the unknown temporal load $G(t)$ in the system

$$\begin{cases} \rho(x)u_{tt} + \mu(x)u_t + (r(x)u_{xx})_{xx} = F(x)G(t), \text{ in } \Omega_T := (0,\ell) \times (0,T), \\ u(x,0) = 0,\ \ u_t(x,0) = 0, \quad x \in (0,\ell), \\ u(0,t) = u_x(0,t) = 0,\ \ r(\ell)u_{xx}(\ell,t) = (r(\ell)u_{xx}(\ell,t))_x = 0,\ \ t \in [0,T], \end{cases}$$

1.1d. ITSP: Other Physical Models

There exist other physical models with the following Dirichlet type measured outputs

Consider the following two basic inverse temporal source problems.

1. Find the unknown temporal load $G(t)$ in the system

$$\begin{cases} \rho(x)u_{tt} + \mu(x)u_t + (r(x)u_{xx})_{xx} = F(x)G(t), \text{ in } \Omega_T := (0,\ell) \times (0,T), \\ u(x,0) = 0, \ \ u_t(x,0) = 0, \quad x \in (0,\ell), \\ u(0,t) = u_x(0,t) = 0, \ \ r(\ell)u_{xx}(\ell,t) = (r(\ell)u_{xx}(\ell,t))_x = 0, \ \ t \in [0,T], \end{cases}$$

2. either from the measured deflection
   $\nu(t) := u(\ell,t), \quad t \in [0,T],$

1.1d. ITSP: Other Physical Models

There exist other physical models with the following Dirichlet type measured outputs

Consider the following two basic inverse temporal source problems.

1. Find the unknown temporal load $G(t)$ in the system

$$\begin{cases} \rho(x)u_{tt} + \mu(x)u_t + (r(x)u_{xx})_{xx} = F(x)G(t), \text{ in } \Omega_T := (0,\ell)\times(0,T), \\ u(x,0)=0,\ \ u_t(x,0)=0, \quad x\in(0,\ell), \\ u(0,t)=u_x(0,t)=0,\ \ r(\ell)u_{xx}(\ell,t)=(r(\ell)u_{xx}(\ell,t))_x=0,\ \ t\in[0,T], \end{cases}$$

2. either from the measured deflection
$\nu(t) := u(\ell,t), \quad t\in[0,T],$
3. or from the measured rotation
$\theta(t) := u_x(\ell,t), \quad t\in[0,T],$
at the right boundary of the cantilever beam.

1.2. Inverse Boundary Value Problems for a Cantilever Beam

Identification of an unknown shear force from measured boundary bending moment

1. in a system governed initial-boundary value problem

$$\begin{cases} \rho(x)u_{tt} + \mu(x)u_t + (r(x)u_{xx})_{xx} = 0, \ (x,t) \in \Omega_T, \\ u(x,0) = 0, \ u_t(x,0) = 0, \quad x \in (0,\ell), \\ u(0,t) = u_x(0,t) = 0, \\ r(\ell)u_{xx}(\ell,t) = 0, \ -(r(\ell)u_{xx}(\ell,t))_x = g(t), \ t \in [0,T], \end{cases} \tag{3}$$

1.2. Inverse Boundary Value Problems for a Cantilever Beam

Identification of an unknown shear force from measured boundary bending moment

1. in a system governed initial-boundary value problem

$$\begin{cases} \rho(x)u_{tt} + \mu(x)u_t + (r(x)u_{xx})_{xx} = 0, \ (x,t) \in \Omega_T, \\ u(x,0) = 0, \ u_t(x,0) = 0, \quad x \in (0,\ell), \\ u(0,t) = u_x(0,t) = 0, \\ r(\ell)u_{xx}(\ell,t) = 0, \quad -(r(\ell)u_{xx}(\ell,t))_x = g(t), \ t \in [0,T], \end{cases} \tag{3}$$

2. from the measured bending moment $\mathcal{M}(t)$ at the left boundary of a beam:

$$\mathcal{M}(t) := -r(0)u_{xx}(0,t), \quad t \in [0,T]. \tag{4}$$

1.2. Inverse Boundary Value Problems for a Cantilever Beam

Identification of an unknown shear force from measured boundary bending moment

1. in a system governed initial-boundary value problem

$$\begin{cases} \rho(x)u_{tt} + \mu(x)u_t + (r(x)u_{xx})_{xx} = 0, \ (x,t) \in \Omega_T, \\ u(x,0) = 0, \ u_t(x,0) = 0, \quad x \in (0,\ell), \\ u(0,t) = u_x(0,t) = 0, \\ r(\ell)u_{xx}(\ell,t) = 0, \quad -(r(\ell)u_{xx}(\ell,t))_x = g(t), \ t \in [0,T], \end{cases} \tag{3}$$

2. from the measured bending moment $\mathcal{M}(t)$ at the left boundary of a beam:

$$\mathcal{M}(t) := -r(0)u_{xx}(0,t), \quad t \in [0,T]. \tag{4}$$

3. This inverse source problem will be defined subsequently as *the Inverse Boundary Balue Problem (IBVP)*

1.2. Inverse Boundary Value Problem: Applications Overview

1. Recent application of microcantilevers in nanotechnology: Transverse Dynamic Force Microscope (TDFM) and Atomic Force Microscope (AFM)

1.2. Inverse Boundary Value Problem: Applications Overview

1. Recent application of microcantilevers in nanotechnology: Transverse Dynamic Force Microscope (TDFM) and Atomic Force Microscope (AFM)
2. The scheme of AFM

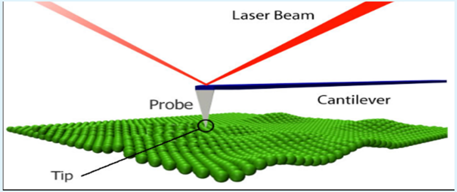

1.2. Inverse Boundary Value Problem: Applications Overview

1. Recent application of microcantilevers in nanotechnology: Transverse Dynamic Force Microscope (TDFM) and Atomic Force Microscope (AFM)
2. The scheme of AFM

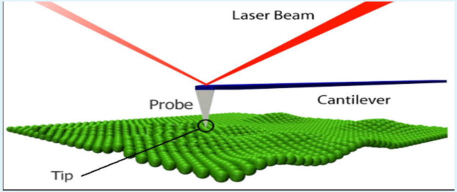

3. **Important references**: M. Antognozzi, *Investigation of the shear force contrast mechanism in transverse dynamic force microscopy*. Ph.D. Thesis, University of Bristol, UK (2000).

1.2. Inverse Boundary Value Problem: Applications Overview

1. Recent application of microcantilevers in nanotechnology: Transverse Dynamic Force Microscope (TDFM) and Atomic Force Microscope (AFM)
2. The scheme of AFM

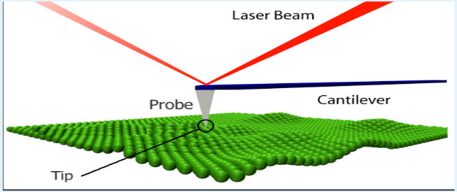

3. **Important references**: M. Antognozzi, *Investigation of the shear force contrast mechanism in transverse dynamic force microscopy*. Ph.D. Thesis, University of Bristol, UK (2000).

1.2. Inverse Boundary Value Problem: Applications Overview

1. Recent application of microcantilevers in nanotechnology: Transverse Dynamic Force Microscope (TDFM) and Atomic Force Microscope (AFM)
2. The scheme of AFM

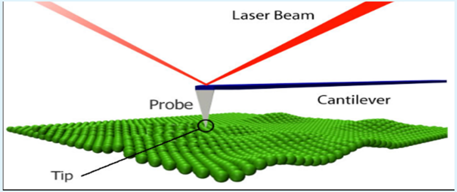

3. **Important references**: M. Antognozzi, *Investigation of the shear force contrast mechanism in transverse dynamic force microscopy*. Ph.D. Thesis, University of Bristol, UK (2000).
4. M. Antognozzi, *et al.* Modeling of cylindrically tapered cantilevers for transverse dynamic force microscopy (TDFM). *Ultramicroscopy, 86*(2001), 223–232.

1.2. Inverse Boundary Value Problem: Applications Overview

1. Recent application of microcantilevers in nanotechnology: Transverse Dynamic Force Microscope (TDFM) and Atomic Force Microscope (AFM)
2. The scheme of AFM

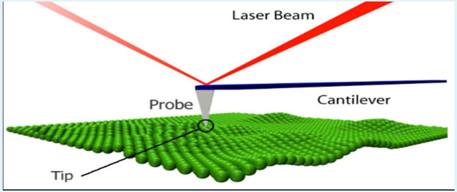

3. **Important references**: M. Antognozzi, *Investigation of the shear force contrast mechanism in transverse dynamic force microscopy*. Ph.D. Thesis, University of Bristol, UK (2000).
4. M. Antognozzi, *et al.* Modeling of cylindrically tapered cantilevers for transverse dynamic force microscopy (TDFM). *Ultramicroscopy, 86*(2001), 223–232.
5. For a simplest (static) Euler-Bernoulli equation, an inverse source problem has been studied in [G. Bao, X. Xu, *Inverse Problems, 29(1)* (015006 (16pp))]

1.2. Inverse Boundary Value Problems: Geometry of the problems

1. Geometry of the IBVP1: *The Neumann-to-Dirichlet map*

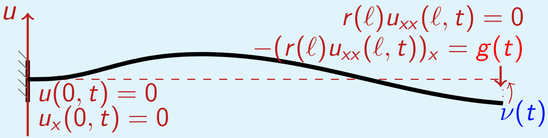

1.2. Inverse Boundary Value Problems: Geometry of the problems

1. Geometry of the IBVP1: *The Neumann-to-Dirichlet map*

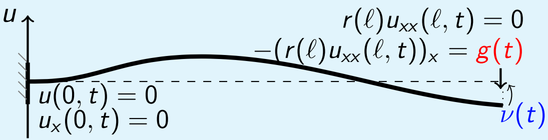

2. Alemdar Hasanov, Onur Baysal and Cristiana Sebu, *Inverse Problems* (2019)

1.2. Inverse Boundary Value Problems: Geometry of the problems

1. Geometry of the IBVP1: *The Neumann-to-Dirichlet map*

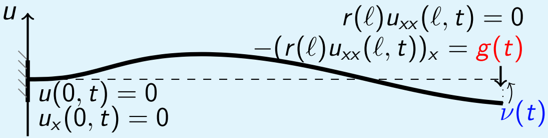

2. Alemdar Hasanov, Onur Baysal and Cristiana Sebu, *Inverse Problems* (2019)
3. Geometry of the IBVP2: *The Neumann-to-Neumann map*

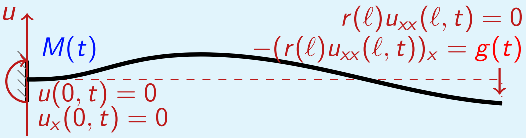

1.2. Inverse Boundary Value Problems: Geometry of the problems

1. Geometry of the IBVP1: *The Neumann-to-Dirichlet map*

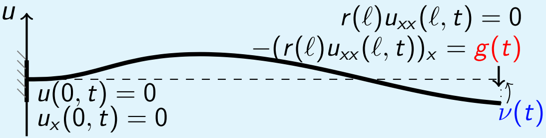

2. Alemdar Hasanov, Onur Baysal and Cristiana Sebu, *Inverse Problems* (2019)
3. Geometry of the IBVP2: *The Neumann-to-Neumann map*

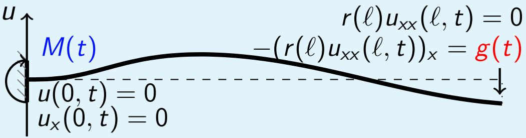

4. IBVP2: Alemdar Hasanov, Onur Baysal and Hiromichi Itou, *Journal of Inverse and Ill-Posed Problems* (2019)

1.3. Inverse Coefficient Problems for a Cantilever Beam

Identification of an unknown principal coefficient(s) $r(x)$ or/and $m(x)$ from measured boundary bending moment

1. Consider the problem of identifying the unknown principal coefficient(s) $r(x)$ or/and $m(x)$ in a system governed initial-boundary value problem

$$\begin{cases} m(x)u_{tt} + \mu(x)u_t + (r(x)u_{xx})_{xx} = 0, \ (x,t) \in \Omega_T, \\ u(x,0) = 0, \ u_t(x,0) = 0, \quad x \in (0,\ell), \\ u(0,t) = u_x(0,t) = 0, \\ r(\ell)u_{xx}(\ell,t) = 0, \quad -(r(\ell)u_{xx}(\ell,t))_x = g(t), \ t \in [0,T], \end{cases} \tag{5}$$

1.3. Inverse Coefficient Problems for a Cantilever Beam

Identification of an unknown principal coefficient(s) $r(x)$ or/and $m(x)$ from measured boundary bending moment

1. Consider the problem of identifying the unknown principal coefficient(s) $r(x)$ or/and $m(x)$ in a system governed initial-boundary value problem

$$\begin{cases} m(x)u_{tt} + \mu(x)u_t + (r(x)u_{xx})_{xx} = 0, \ (x,t) \in \Omega_T, \\ u(x,0) = 0, \ u_t(x,0) = 0, \quad x \in (0,\ell), \\ u(0,t) = u_x(0,t) = 0, \\ r(\ell)u_{xx}(\ell,t) = 0, \quad -(r(\ell)u_{xx}(\ell,t))_x = g(t), \ t \in [0,T], \end{cases} \tag{5}$$

2. from the measured deflection $\nu(t) := u(\ell, t)$ at the right boundary $x = \ell$ of a beam,

1.3. Inverse Coefficient Problems for a Cantilever Beam

Identification of an unknown principal coefficient(s) $r(x)$ or/and $m(x)$ from measured boundary bending moment

1. Consider the problem of identifying the unknown principal coefficient(s) $r(x)$ or/and $m(x)$ in a system governed initial-boundary value problem

$$\begin{cases} m(x)u_{tt} + \mu(x)u_t + (r(x)u_{xx})_{xx} = 0, \ (x,t) \in \Omega_T, \\ u(x,0) = 0, \ u_t(x,0) = 0, \quad x \in (0,\ell), \\ u(0,t) = u_x(0,t) = 0, \\ r(\ell)u_{xx}(\ell,t) = 0, \quad -(r(\ell)u_{xx}(\ell,t))_x = g(t), \ t \in [0,T], \end{cases} \tag{5}$$

2. from the measured deflection $\nu(t) := u(\ell,t)$ at the right boundary $x = \ell$ of a beam,
3. or/and from the measured bending moment $\mathcal{M}(t) := -r(0)u_{xx}(0,t)$, $t \in [0,T]$, at the left boundary $x = 0$ of a beam.

2.1. Classification of main methods/approaches

1. From the **point of view of methods/approaches used**, the recent studies on the inverse and parameter identification problems for the dynamic Euler-Bernoulli equation can be broadly divided into **two groups**:

2.1. Classification of main methods/approaches

1. From the **point of view of methods/approaches used**, the recent studies on the inverse and parameter identification problems for the dynamic Euler-Bernoulli equation can be broadly divided into **two groups**:
2. *methods based on spectral theory differential operators*

2.1. Classification of main methods/approaches

1. From the **point of view of methods/approaches used**, the recent studies on the inverse and parameter identification problems for the dynamic Euler-Bernoulli equation can be broadly divided into **two groups**:
2. *methods based on spectral theory differential operators*
3. See,
   V. Barcilon, Geoph. J. of the Royal Astronomical Society (1974)].
   V. Barcilon, Philosophical Trans. of the Royal Society of London (1982)
   J. R. McLaughlin, SIAM J. of Math. Analysis (1976)
   G. M.L. Gladwell, Proc. of the Royal Society (1986).

2.1. Classification of main methods/approaches

1. From the **point of view of methods/approaches used**, the recent studies on the inverse and parameter identification problems for the dynamic Euler-Bernoulli equation can be broadly divided into **two groups**:
2. *methods based on spectral theory differential operators*
3. See,
   V. Barcilon, Geoph. J. of the Royal Astronomical Society (1974)].
   V. Barcilon, Philosophical Trans. of the Royal Society of London (1982)
   J. R. McLaughlin, SIAM J. of Math. Analysis (1976)
   G. M.L. Gladwell, Proc. of the Royal Society (1986).
4. and *methods based on control theory for PDEs*

2.1. Classification of main methods/approaches

1. From the **point of view of methods/approaches used**, the recent studies on the inverse and parameter identification problems for the dynamic Euler-Bernoulli equation can be broadly divided into **two groups**:
2. *methods based on spectral theory differential operators*
3. See,
   V. Barcilon, Geoph. J. of the Royal Astronomical Society (1974)].
   V. Barcilon, Philosophical Trans. of the Royal Society of London (1982)
   J. R. McLaughlin, SIAM J. of Math. Analysis (1976)
   G. M.L. Gladwell, Proc. of the Royal Society (1986).
4. and *methods based on control theory for PDEs*
5. See,
   S. Nicaise, O. Zair, Electronic Journal of Differential Equations, 20 (2004)
   J-D. Chang and B.Z. Guo, Automatica (2007)

2.2. Classification of main methods/approaches: methods based on spectral theory

1. Inverse coefficient problems related to the determination of properties (rigidity or density distributions) of a beam from the knowledge of *spectral information* have been studied beginning from the pioneering work of Barcilon [V. Barcilon, *Geoph. J. of the Royal Astronomical Society* (1974)].

2.2. Classification of main methods/approaches: methods based on spectral theory

1. Inverse coefficient problems related to the determination of properties (rigidity or density distributions) of a beam from the knowledge of *spectral information* have been studied beginning from the pioneering work of Barcilon [V. Barcilon, *Geoph. J. of the Royal Astronomical Society* (1974)].
2. These methods are then developed by many distinguished mathematicians ([V. Barcilon, *Philosophical Trans. of the Royal Society of London* (1982)], [J. R. McLaughlin, *SIAM J. of Math. Analysis* (1976)], [G. M. L. Gladwell, *Proc. of the Royal Society* (1986)]).

2.2. Classification of main methods/approaches: methods based on spectral theory

1. Inverse coefficient problems related to the determination of properties (rigidity or density distributions) of a beam from the knowledge of *spectral information* have been studied beginning from the pioneering work of Barcilon [V. Barcilon, *Geoph. J. of the Royal Astronomical Society* (1974)].
2. These methods are then developed by many distinguished mathematicians ([V. Barcilon, *Philosophical Trans. of the Royal Society of London* (1982)], [J. R. McLaughlin, *SIAM J. of Math. Analysis* (1976)], [G. M. L. Gladwell, *Proc. of the Royal Society* (1986)]).
3. These problems and methods have received much attention in scientific literature for many years not only because of mathematical importance, but also because of wide range of applications.

2.3. The main uniqueness result: the spectral method

1. It was shown, first in [Barcilon,1982] and then in [Gladwell, 1986], that three complete spectra, corresponding to three different boundary conditions at one end of the beam are necessary and sufficient for the reconstruction of the cross-sectional area $A(x)$ and the moment of area about the neural axis (or moment of inertia of a shape) $I(x)$ in the (undamped) Euler–Bernoulli equation $\rho A(x)u_{tt} + (E\,I(x)u_{xx})_{xx} = 0$.

2.3. The main uniqueness result: the spectral method

1. It was shown, first in [Barcilon,1982] and then in [Gladwell, 1986], that three complete spectra, corresponding to three different boundary conditions at one end of the beam are necessary and sufficient for the reconstruction of the cross-sectional area $A(x)$ and the moment of area about the neural axis (or moment of inertia of a shape) $I(x)$ in the (undamped) Euler–Bernoulli equation $\rho A(x)u_{tt} + (E\,I(x)u_{xx})_{xx} = 0$.
2. All these uniqeness results are based on the reconstruction technique due to [Mclaughlin, 1986], which is, in turn, is based on the well-known Gel'fand-Levitan reconstruction procedure for the potential in the Sturm-Liouville equation [I. M. Gel'fand, B. M. Levitan, On the determination of a differential equation from its special function, *Izv. Akad. Nauk SSR., Ser. Mat. 15*(1951), 309–360 (Russian); English transl. in *Amer. Math. Soc. Transl. Ser. 2 (1)*, 253–304]

2.3. The main uniqueness result: the spectral method

1. It was shown, first in [Barcilon,1982] and then in [Gladwell, 1986], that three complete spectra, corresponding to three different boundary conditions at one end of the beam are necessary and sufficient for the reconstruction of the cross-sectional area $A(x)$ and the moment of area about the neural axis (or moment of inertia of a shape) $I(x)$ in the (undamped) Euler–Bernoulli equation $\rho A(x)u_{tt} + (E\,I(x)u_{xx})_{xx} = 0$.
2. All these uniqeness results are based on the reconstruction technique due to [Mclaughlin, 1986], which is, in turn, is based on the well-known Gel'fand-Levitan reconstruction procedure for the potential in the Sturm-Liouville equation [I. M. Gel'fand, B. M. Levitan, On the determination of a differential equation from its special function, *Izv. Akad. Nauk SSR., Ser. Mat. 15*(1951), 309–360 (Russian); English transl. in *Amer. Math. Soc. Transl. Ser. 2 (1)*, 253–304]
3. However, it has been found that in practice it is difficult to acquire spectral data.

2.3. The main uniqueness result: methods based on control theory

1. Assuming that the coefficients are smooth enough, i.e. $m, r \in C^4(0, \ell)$ and the time interval is infinite, i.e. $t \in (0, \infty)$, to allow the use of the Laplace transform,

2.3. The main uniqueness result: methods based on control theory

1. Assuming that the coefficients are smooth enough, i.e. $m, r \in C^4(0,\ell)$ and the time interval is infinite, i.e. $t \in (0,\infty)$, to allow the use of the Laplace transform,
2. it was proved that the unknown coefficients $m(x)$ and $r(x)$ in

$$\begin{cases} m(x)u_{tt} + (r(x)u_{xx})_{xx} = 0, \; x \in (0,\ell), \; t > 0, \\ u(x,0) = 0, \; u_t(x,0) = 0, \;\; x \in (0,\ell), \\ u(0,t) = u_x(0,t) = 0, \\ u_{xx}(x,t)|_{x=\ell} = 0, \; (r(x)u_{xx}(x,t))_x|_{x=\ell} = g(t), \; t > 0, \end{cases}$$

2.3. The main uniqueness result: methods based on control theory

1. Assuming that the coefficients are smooth enough, i.e. $m, r \in C^4(0,\ell)$ and the time interval is infinite, i.e. $t \in (0,\infty)$, to allow the use of the Laplace transform,
2. it was proved that the unknown coefficients $m(x)$ and $r(x)$ in

$$\begin{cases} m(x)u_{tt} + (r(x)u_{xx})_{xx} = 0, \ x \in (0,\ell), \ t > 0, \\ u(x,0) = 0, \ u_t(x,0) = 0, \ \ x \in (0,\ell), \\ u(0,t) = u_x(0,t) = 0, \\ u_{xx}(x,t)|_{x=\ell} = 0, \ (r(x)u_{xx}(x,t))_x|_{x=\ell} = g(t), \ t > 0, \end{cases}$$

3. can be uniquely determined from the given boundary measured outputs $\nu(t) := u(\ell,t)$ (deflection at $x = l$) and $\theta(t) := u_x(\ell,t)$ (slope at $x = \ell$), available for all $t > 0$.

2.3. The main uniqueness result: methods based on control theory

1. Assuming that the coefficients are smooth enough, i.e. $m, r \in C^4(0,\ell)$ and the time interval is infinite, i.e. $t \in (0,\infty)$, to allow the use of the Laplace transform,
2. it was proved that the unknown coefficients $m(x)$ and $r(x)$ in

$$\begin{cases} m(x)u_{tt} + (r(x)u_{xx})_{xx} = 0, \; x \in (0,\ell), \; t > 0, \\ u(x,0) = 0, \; u_t(x,0) = 0, \quad x \in (0,\ell), \\ u(0,t) = u_x(0,t) = 0, \\ u_{xx}(x,t)|_{x=\ell} = 0, \; (r(x)u_{xx}(x,t))_x|_{x=\ell} = g(t), \; t > 0, \end{cases}$$

3. can be uniquely determined from the given boundary measured outputs $\nu(t) := u(\ell,t)$ (deflection at $x = l$) and $\theta(t) := u_x(\ell,t)$ (slope at $x = \ell$), available for all $t > 0$.
4. This fundamental result bridged the gap between the above mentioned two methods.

2.3. The main uniqueness result: methods based on control theory

1. Assuming that the coefficients are smooth enough, i.e. $m, r \in C^4(0,\ell)$ and the time interval is infinite, i.e. $t \in (0,\infty)$, to allow the use of the Laplace transform,
2. it was proved that the unknown coefficients $m(x)$ and $r(x)$ in

$$\begin{cases} m(x)u_{tt} + (r(x)u_{xx})_{xx} = 0, \; x \in (0,\ell), \; t > 0, \\ u(x,0) = 0, \; u_t(x,0) = 0, \quad x \in (0,\ell), \\ u(0,t) = u_x(0,t) = 0, \\ u_{xx}(x,t)|_{x=\ell} = 0, \; (r(x)u_{xx}(x,t))_x|_{x=\ell} = g(t), \; t > 0, \end{cases}$$

3. can be uniquely determined from the given boundary measured outputs $\nu(t) := u(\ell,t)$ (deflection at $x = l$) and $\theta(t) := u_x(\ell,t)$ (slope at $x = \ell$), available for all $t > 0$.
4. This fundamental result bridged the gap between the above mentioned two methods.
5. However, the drawback of this method is that in real engineering models the *time interval is finite and may be small enough*, since the information propagation speed in elastic beams is not finite [L.D. Landau, E.M. Lifshitz, *Theory of Elasticity*, 3rd edn., New-York: Butterworth-Heinemann (1986)].

3.1. Distinguished Features of the Considered Classes of Inverse Problems

1. The Euler-Bernoulli equation includes all the physical (variable) coefficients.

3.1. Distinguished Features of the Considered Classes of Inverse Problems

1. The Euler-Bernoulli equation includes all the physical (variable) coefficients.
2. The time interval is finite and the final time $T > 0$ may be small enough.

3.1. Distinguished Features of the Considered Classes of Inverse Problems

1. The Euler-Bernoulli equation includes all the physical (variable) coefficients.
2. The time interval is finite and the final time $T > 0$ may be small enough.
3. All the inverse problems are based only on available boundary measured output(s).

3.1. Distinguished Features of the Considered Classes of Inverse Problems

1. The Euler-Bernoulli equation includes all the physical (variable) coefficients.
2. The time interval is finite and the final time $T > 0$ may be small enough.
3. All the inverse problems are based only on available boundary measured output(s).
4. Namely, the measured outputs are: boundary deflection, slope or/and moment.

3.2. Methodology of the Proposed Approaches

1. The proposed approach is based;

3.2. Methodology of the Proposed Approaches

1. The proposed approach is based;
2. on the weak solution theory for PDEs,

3.2. Methodology of the Proposed Approaches

1. The proposed approach is based;
2. on the weak solution theory for PDEs,
3. analysis of input-output operators,

3.2. Methodology of the Proposed Approaches

1. The proposed approach is based;
2. on the weak solution theory for PDEs,
3. analysis of input-output operators,
4. Tikhonov regularization combined with the adjoint method,

3.2. Methodology of the Proposed Approaches

1. The proposed approach is based;
2. on the weak solution theory for PDEs,
3. analysis of input-output operators,
4. Tikhonov regularization combined with the adjoint method,
5. Hermite Finite Element Method for discretization of the direct problem

3.2. Methodology of the Proposed Approaches

1. The proposed approach is based;
2. on the weak solution theory for PDEs,
3. analysis of input-output operators,
4. Tikhonov regularization combined with the adjoint method,
5. Hermite Finite Element Method for discretization of the direct problem
6. Conjugate Gradient Algorithm with explicit Fréchet gradient formula

3.3. Distinguished Features of the Proposed Approaches

1. This proposed approach requires minimal smoothness from the inputs which is important in real engineering applications;

3.3. Distinguished Features of the Proposed Approaches

1. This proposed approach requires minimal smoothness from the inputs which is important in real engineering applications;
2. It allows to find out the main properties of the Dirichlet-to-Neumann and Neumann-to-Neumann operators corresponding to all the three classes of inverse problems;

3.3. Distinguished Features of the Proposed Approaches

1. This proposed approach requires minimal smoothness from the inputs which is important in real engineering applications;
2. It allows to find out the main properties of the Dirichlet-to-Neumann and Neumann-to-Neumann operators corresponding to all the three classes of inverse problems;
3. It establishes the relationship between the regularity of the weak solution of the direct problem and the type (Dirichlet or Neumann) of measured output;

3.3. Distinguished Features of the Proposed Approaches

1. This proposed approach requires minimal smoothness from the inputs which is important in real engineering applications;
2. It allows to find out the main properties of the Dirichlet-to-Neumann and Neumann-to-Neumann operators corresponding to all the three classes of inverse problems;
3. It establishes the relationship between the regularity of the weak solution of the direct problem and the type (Dirichlet or Neumann) of measured output;
4. The approach allows to prove existence, and in some cases, the uniqueness of a solution;

3.3. Distinguished Features of the Proposed Approaches

1. This proposed approach requires minimal smoothness from the inputs which is important in real engineering applications;
2. It allows to find out the main properties of the Dirichlet-to-Neumann and Neumann-to-Neumann operators corresponding to all the three classes of inverse problems;
3. It establishes the relationship between the regularity of the weak solution of the direct problem and the type (Dirichlet or Neumann) of measured output;
4. The approach allows to prove existence, and in some cases, the uniqueness of a solution;
5. It permits to derive an explicit Fréchet gradient formula for all the above formulated inverse problems;

3.3. Distinguished Features of the Proposed Approaches

1. This proposed approach requires minimal smoothness from the inputs which is important in real engineering applications;
2. It allows to find out the main properties of the Dirichlet-to-Neumann and Neumann-to-Neumann operators corresponding to all the three classes of inverse problems;
3. It establishes the relationship between the regularity of the weak solution of the direct problem and the type (Dirichlet or Neumann) of measured output;
4. The approach allows to prove existence, and in some cases, the uniqueness of a solution;
5. It permits to derive an explicit Fréchet gradient formula for all the above formulated inverse problems;
6. Due to this circumstance, it is possible to develop efficient (i.e. fast and with high accuracy) numerical algorithms.

4.1. The Main Conditions and the Set of Admissible Inputs

1. In all inverse problems we assume that the functions $\rho(x)$, $\mu(x)$ and $r(x)$ satisfy the following conditions:

4.1. The Main Conditions and the Set of Admissible Inputs

1. In all inverse problems we assume that the functions $\rho(x)$, $\mu(x)$ and $r(x)$ satisfy the following conditions:
2. (defined as the *main conditions*)

$$\begin{cases} \rho, r, \mu \in L^{\infty}(0, l), \\ 0 < \rho_0 \leq \rho(x) \leq \rho_1, \; 0 < r_0 \leq r(x) \leq r_1, \\ 0 < \mu_0 \leq \mu(x) \leq \mu_1. \end{cases}$$

4.1. The Main Conditions and the Set of Admissible Inputs

1. In all inverse problems we assume that the functions $\rho(x)$, $\mu(x)$ and $r(x)$ satisfy the following conditions:
2. (defined as the *main conditions*)

$$\begin{cases} \rho, r, \mu \in L^{\infty}(0, l), \\ 0 < \rho_0 \leq \rho(x) \leq \rho_1, \; 0 < r_0 \leq r(x) \leq r_1, \\ 0 < \mu_0 \leq \mu(x) \leq \mu_1. \end{cases}$$

3. We introduce the set of *admissible inputs*,

4.1. The Main Conditions and the Set of Admissible Inputs

1. In all inverse problems we assume that the functions $\rho(x)$, $\mu(x)$ and $r(x)$ satisfy the following conditions:
2. (defined as the *main conditions*)

$$\begin{cases} \rho, r, \mu \in L^{\infty}(0,l), \\ 0 < \rho_0 \leq \rho(x) \leq \rho_1, \; 0 < r_0 \leq r(x) \leq r_1, \\ 0 < \mu_0 \leq \mu(x) \leq \mu_1. \end{cases}$$

3. We introduce the set of *admissible inputs*,
4. i.e admissible temporal loads

$$\mathbf{G}^k := \{G \in H^k(0,T): \; \|G\|_{H^k(0,T)} \leq \gamma\}, \; \gamma > 0, \; k = 1,2,3.$$

4.2. Inverse Temporal Source Problem (ITSP)

1. Find $G \in \mathbf{G}^k$

4.2. Inverse Temporal Source Problem (ITSP)

1. Find $G \in \mathbf{G}^k$
2. in

$$\left\{ \begin{array}{l} \left\{ \begin{array}{l} \rho(x)u_{tt} + \mu(x)u_t + (r(x)u_{xx})_{xx} = F(x)G(t), \text{ in } \Omega_T := (0,\ell) \times (0,T), \\ u(x,0) = 0,\ u_t(x,0) = 0, \quad x \in (0,\ell), \\ u(0,t) = u_x(0,t) = 0,\ r(\ell)u_{xx}(\ell,t) = (r(\ell)u_{xx}(\ell,t))_x = 0,\ t \in [0,T], \end{array} \right. \\ -r(0)u_{xx}(0,t) = \mathcal{M}(t), \quad t \in [0,T]. \end{array} \right.$$

4.2. Inverse Temporal Source Problem (ITSP)

1. Find $G \in \mathbf{G}^k$
2. in

$$\left\{ \begin{array}{l} \left\{ \begin{array}{l} \rho(x)u_{tt} + \mu(x)u_t + (r(x)u_{xx})_{xx} = F(x)G(t), \text{ in } \Omega_T := (0,\ell) \times (0,T), \\ u(x,0) = 0,\ u_t(x,0) = 0,\quad x \in (0,\ell), \\ u(0,t) = u_x(0,t) = 0,\ r(\ell)u_{xx}(\ell,t) = (r(\ell)u_{xx}(\ell,t))_x = 0,\ t \in [0,T], \end{array} \right. \\ -r(0)u_{xx}(0,t) = \mathcal{M}(t),\quad t \in [0,T]. \end{array} \right.$$

3. We introduce the *input-output operator* defined on $\mathcal{G}^k$ as follows:

$$(\Psi G)(t) := -r(0)u_{xx}(0,t;G),\ t \in (0,T).$$

4.2. Inverse Temporal Source Problem (ITSP)

1. Find $G \in \mathbf{G}^k$
2. in

$$\left\{ \begin{array}{l} \left\{ \begin{array}{l} \rho(x)u_{tt} + \mu(x)u_t + (r(x)u_{xx})_{xx} = F(x)G(t), \text{ in } \Omega_T := (0,\ell) \times (0,T), \\ u(x,0) = 0, \;\; u_t(x,0) = 0, \;\;\; x \in (0,\ell), \\ u(0,t) = u_x(0,t) = 0, \;\; r(\ell)u_{xx}(\ell,t) = (r(\ell)u_{xx}(\ell,t))_x = 0, \;\; t \in [0,T], \end{array} \right. \\ -r(0)u_{xx}(0,t) = \mathcal{M}(t), \;\;\; t \in [0,T]. \end{array} \right.$$

3. We introduce the *input-output operator* defined on $\mathcal{G}^k$ as follows:

$$(\Psi G)(t) := -r(0)u_{xx}(0,t;G), \;\; t \in (0,T).$$

4. and reformulate the inverse problem as the linear operator equation

$$(\Psi G)(t) = \mathcal{M}(t), \;\;\; t \in (0,T).$$

4.3. The ITSP: Properties of the Input-Output Operator

1. The compactness class for the input-output operator

4.3. The ITSP: Properties of the Input-Output Operator

1. The compactness class for the input-output operator
2. **Lemma 4.1.** Assume that the main conditions hold and $G \in \mathbf{G}^2$. Then the input-output map $\Psi[\cdot] : \mathbf{G}^2 \mapsto L^2(0, T)$ defined on the admissible set of regular inputs $\mathbf{G}^2 \subset H^2(0, T)$ is a linear compact operator.

4.3. The ITSP: Properties of the Input-Output Operator

1. The compactness class for the input-output operator
2. **Lemma 4.1.** Assume that the main conditions hold and $G \in \mathbf{G}^2$. Then the input-output map $\Psi[\cdot] : \mathbf{G}^2 \mapsto L^2(0, T)$ defined on the admissible set of regular inputs $\mathbf{G}^2 \subset H^2(0, T)$ is a linear compact operator.
3. Compactness of the input-output operator implies that *the ITSP is ill-posed*

4.3. The ITSP: Properties of the Input-Output Operator

1. The compactness class for the input-output operator
2. **Lemma 4.1.** Assume that the main conditions hold and $G \in \mathbf{G}^2$. Then the input-output map $\Psi[\cdot] : \mathbf{G}^2 \mapsto L^2(0, T)$ defined on the admissible set of regular inputs $\mathbf{G}^2 \subset H^2(0, T)$ is a linear compact operator.
3. Compactness of the input-output operator implies that *the ITSP is ill-posed*
4. The Lipschitz continuity of the input-output operator

4.3. The ITSP: Properties of the Input-Output Operator

1. The compactness class for the input-output operator
2. **Lemma 4.1.** Assume that the main conditions hold and $G \in \mathbf{G}^2$. Then the input-output map $\Psi[\cdot] : \mathbf{G}^2 \mapsto L^2(0,T)$ defined on the admissible set of regular inputs $\mathbf{G}^2 \subset H^2(0,T)$ is a linear compact operator.
3. Compactness of the input-output operator implies that *the ITSP is ill-posed*
4. The Lipschitz continuity of the input-output operator
5. **Lemma 4.2.** Assume that the main conditions hold and $G \in \mathbf{G}^1$. Then the input-output operator $\Psi[\cdot] : \mathbf{G}^1 \mapsto L^2(0,T)$ defined on the admissible set of extended inputs $\mathbf{G}^1 \subset H^1(0,T)$ is Lipschitz continuous, that is

$$\|\Psi G_1 - \Psi G_2\|_{L^2(0,T)} \leq L_\Psi \|G_1 - G_2\|_{H^1(0,T)},$$

for all $G_1, G_2 \in \mathbf{G}$,

4.3. The ITSP: Properties of the Input-Output Operator

1. The compactness class for the input-output operator
2. **Lemma 4.1.** Assume that the main conditions hold and $G \in \mathbf{G}^2$. Then the input-output map $\Psi[\cdot] : \mathbf{G}^2 \mapsto L^2(0,T)$ defined on the admissible set of regular inputs $\mathbf{G}^2 \subset H^2(0,T)$ is a linear compact operator.
3. Compactness of the input-output operator implies that *the ITSP is ill-posed*
4. The Lipschitz continuity of the input-output operator
5. **Lemma 4.2.** Assume that the main conditions hold and $G \in \mathbf{G}^1$. Then the input-output operator $\Psi[\cdot] : \mathbf{G}^1 \mapsto L^2(0,T)$ defined on the admissible set of extended inputs $\mathbf{G}^1 \subset H^1(0,T)$ is Lipschitz continuous, that is

$$\|\Psi G_1 - \Psi G_2\|_{L^2(0,T)} \leq L_\Psi \|G_1 - G_2\|_{H^1(0,T)},$$

for all $G_1, G_2 \in \mathbf{G}$,

6. with the Lipschitz constant $L_\Psi > 0$ depending only on the constants in the main conditions and on the norm $\|F\|_{L^2(0,l)}$.

4.4. The ITSP: Existence of a Quasisolution

1. Due to random noise in $\mathcal{M}(t)$ an exact equality in $(\Psi G)(t) = \mathcal{M}(t)$ is never possible.

4.4. The ITSP: Existence of a Quasisolution

1. Due to random noise in $\mathcal{M}(t)$ an exact equality in $(\Psi G)(t) = \mathcal{M}(t)$ is never possible.
2. Hence one needs to introduce the Tikhonov functional

$$J(G) = \frac{1}{2}\|r(0)u_{xx}(0,\cdot;G) + \mathcal{M}\|^2_{L^2(0,T)}, \ \ G \in \mathbf{G}^1 \subset H^1(0,T)$$

4.4. The ITSP: Existence of a Quasisolution

1. Due to random noise in $\mathcal{M}(t)$ an exact equality in $(\Psi G)(t) = \mathcal{M}(t)$ is never possible.
2. Hence one needs to introduce the Tikhonov functional

$$J(G) = \frac{1}{2}\|r(0)u_{xx}(0,\cdot;G) + \mathcal{M}\|^2_{L^2(0,T)}, \;\; G \in \mathbf{G}^1 \subset H^1(0,T)$$

3. and reformulate the ITSP as the following minimization problem

$$J(G_*) = \inf_{G \in \mathbf{G}^1} J(G).$$

4.4. The ITSP: Existence of a Quasisolution

1. Due to random noise in $\mathcal{M}(t)$ an exact equality in $(\Psi G)(t) = \mathcal{M}(t)$ is never possible.
2. Hence one needs to introduce the Tikhonov functional

$$J(G) = \frac{1}{2} \| r(0) u_{xx}(0, \cdot; G) + \mathcal{M} \|^2_{L^2(0,T)}, \;\; G \in \mathbf{G}^1 \subset H^1(0, T)$$

3. and reformulate the ITSP as the following minimization problem

$$J(G_*) = \inf_{G \in \mathbf{G}^1} J(G).$$

4. A solution of this minimization is defined as a quasi-solution of the ITSP.

4.4. The ITSP: Existence of a Quasisolution

1. Due to random noise in $\mathcal{M}(t)$ an exact equality in $(\Psi G)(t) = \mathcal{M}(t)$ is never possible.
2. Hence one needs to introduce the Tikhonov functional

$$J(G) = \frac{1}{2} \| r(0) u_{xx}(0, \cdot; G) + \mathcal{M} \|^2_{L^2(0,T)}, \; G \in \mathbf{G}^1 \subset H^1(0, T)$$

3. and reformulate the ITSP as the following minimization problem

$$J(G_*) = \inf_{G \in \mathbf{G}^1} J(G).$$

4. A solution of this minimization is defined as a quasi-solution of the ITSP.
5. **Theorem 4.1.** *Assume that the main conditions hold and $G \in \mathbf{G}^1$. Then the minimization problem has a solution in $\mathbf{G}^1 \subset H^1(0, T)$.*

4.4. The ITSP: Existence of a Quasisolution

1. Due to random noise in $\mathcal{M}(t)$ an exact equality in $(\Psi G)(t) = \mathcal{M}(t)$ is never possible.
2. Hence one needs to introduce the Tikhonov functional

$$J(G) = \frac{1}{2}\|r(0)u_{xx}(0,\cdot;G) + \mathcal{M}\|^2_{L^2(0,T)}, \; G \in \mathbf{G}^1 \subset H^1(0,T)$$

3. and reformulate the ITSP as the following minimization problem

$$J(G_*) = \inf_{G \in \mathbf{G}^1} J(G).$$

4. A solution of this minimization is defined as a quasi-solution of the ITSP.
5. **Theorem 4.1.** *Assume that the main conditions hold and $G \in \mathbf{G}^1$. Then the minimization problem has a solution in $\mathbf{G}^1 \subset H^1(0,T)$.*
6. This thoeorem implies the existence of a quasi-solution of the ITSP in $\mathbf{G}^1 \subset H^1(0,T)$.
7. **Remark 4.1.** The regularized Tikhonov functional $J_\alpha(G) = J(G) + \alpha\|G\|^2_{H^1(0,T)}$ has a unique minimum $G_\alpha \in \mathbf{G}^1$ provided that the conditions od Theorem 4.1 hold.

4.5(a). The ITSP: Fréchet Gradient of the Tikhonov Functional

1. **The main integral relationship**

4.5(a). The ITSP: Fréchet Gradient of the Tikhonov Functional

1. **The main integral relationship**
2. **Lemma 4.3.** Assume that the main conditions hold and $G \in \mathbf{G}^1$.

4.5(a). The ITSP: Fréchet Gradient of the Tikhonov Functional

1. **The main integral relationship**
2. **Lemma 4.3.** Assume that the main conditions hold and $G \in \mathbf{G}^1$.
3. Then the following integral relationship holds:

$$\int_0^T r(0)\delta u_{xx}(0,t)\, p(t)dt = \int_0^T \left(\int_0^l F(x)\phi(x,t)dx \right) \delta G(t)dt, \;\; G, \delta G \in \mathbf{G}^1,$$

4.5(a). The ITSP: Fréchet Gradient of the Tikhonov Functional

1. **The main integral relationship**
2. **Lemma 4.3.** Assume that the main conditions hold and $G \in \mathbf{G}^1$.
3. Then the following integral relationship holds:

$$\int_0^T r(0)\delta u_{xx}(0,t)\, p(t)dt = \int_0^T \left(\int_0^l F(x)\phi(x,t)dx \right) \delta G(t)dt, \;\; G, \delta G \in \mathbf{G}^1,$$

4. where $\phi(x,t)$ is the solution of the adjoint problem

$$\begin{cases} \rho(x)\phi_{tt} - \mu(x)\phi_t + (r(x)\phi_{xx})_{xx} = 0, \;\; (x,t) \in \Omega_T, \\ \phi(x,T) = 0, \;\; \phi_t(x,T) = 0, \quad x \in (0,l), \\ \phi(0,t) = 0, \;\; \phi_x(0,t) = p(t), \;\; t \in [0,T], \\ \phi_{xx}(l,t) = 0, \quad -(r(l)\phi_{xx}(l,t))_x = 0, \;\; t \in [0,T], \end{cases}$$

4.5(a). The ITSP: Fréchet Gradient of the Tikhonov Functional

1. **The main integral relationship**
2. **Lemma 4.3.** Assume that the main conditions hold and $G \in \mathbf{G}^1$.
3. Then the following integral relationship holds:

$$\int_0^T r(0)\delta u_{xx}(0,t)\, p(t)dt = \int_0^T \left(\int_0^l F(x)\phi(x,t)dx \right) \delta G(t)dt, \;\; G, \delta G \in \mathbf{G}^1,$$

4. where $\phi(x,t)$ is the solution of the adjoint problem

$$\begin{cases} \rho(x)\phi_{tt} - \mu(x)\phi_t + (r(x)\phi_{xx})_{xx} = 0, \;\; (x,t) \in \Omega_T, \\ \phi(x,T) = 0, \;\; \phi_t(x,T) = 0, \quad x \in (0,l), \\ \phi(0,t) = 0, \;\; \phi_x(0,t) = p(t), \;\; t \in [0,T], \\ \phi_{xx}(l,t) = 0, \quad -(r(l)\phi_{xx}(l,t))_x = 0, \;\; t \in [0,T], \end{cases}$$

5. with the arbitrary input $p \in L^2(0,T)$.

4.5(a). The ITSP: Fréchet Gradient of the Tikhonov Functional

1. **The main integral relationship**
2. **Lemma 4.3.** Assume that the main conditions hold and $G \in \mathbf{G}^1$.
3. Then the following integral relationship holds:

$$\int_0^T r(0)\delta u_{xx}(0,t)\, p(t)dt = \int_0^T \left(\int_0^l F(x)\phi(x,t)dx \right) \delta G(t)dt, \;\; G, \delta G \in \mathbf{G}^1,$$

4. where $\phi(x,t)$ is the solution of the adjoint problem

$$\begin{cases} \rho(x)\phi_{tt} - \mu(x)\phi_t + (r(x)\phi_{xx})_{xx} = 0, \;\; (x,t) \in \Omega_T, \\ \phi(x,T) = 0, \;\; \phi_t(x,T) = 0, \quad x \in (0,l), \\ \phi(0,t) = 0, \;\; \phi_x(0,t) = p(t), \;\; t \in [0,T], \\ \phi_{xx}(l,t) = 0, \quad -(r(l)\phi_{xx}(l,t))_x = 0, \;\; t \in [0,T], \end{cases}$$

5. with the arbitrary input $p \in L^2(0,T)$.
6. This integral identity reveals the input-output relationship through the weak solution of the adjoint problem corresponding to the ITSP.

4.5(b). The ITSP: The Increment Formula

1. We choose *formally* the arbitrary input $\theta(t)$ in the adjoint problem as follows:

$$p(t) = r(0)u_{xx}(0, t) + \mathcal{M}(t), \;\; t \in [0, T].$$

4.5(b). The ITSP: The Increment Formula

1. We choose *formally* the arbitrary input $\theta(t)$ in the adjoint problem as follows:

$$p(t) = r(0)u_{xx}(0,t) + \mathcal{M}(t), \;\; t \in [0,T].$$

2. In view of the increment formula

$$\delta J(G) = \int_0^T [r(0)u_{xx}(0,t) + \mathcal{M}(t)]\,(r(0)\delta u_{xx}(0,t))\,dt + \frac{1}{2}\int_0^T [r(0)\delta u_{xx}(0,t)]^2\,dt$$

and the above integral relationship this implies:

$$\delta J(G) = \int_0^T \left(\int_0^l F(x)\phi(x,t)dx \right) \delta G(t)dt + \frac{1}{2}\int_0^T [r(0)\delta u_{xx}(0,t)]^2\,dt.$$

4.5(b). The ITSP: The Increment Formula

1. We choose *formally* the arbitrary input $\theta(t)$ in the adjoint problem as follows:

$$p(t) = r(0)u_{xx}(0, t) + \mathcal{M}(t), \;\; t \in [0, T].$$

2. In view of the increment formula

$$\delta J(G) = \int_0^T \left[r(0)u_{xx}(0, t) + \mathcal{M}(t)\right] \left(r(0)\delta u_{xx}(0, t)\right) dt + \frac{1}{2}\int_0^T \left[r(0)\delta u_{xx}(0, t)\right]^2 dt$$

and the above integral relationship this implies:

$$\delta J(G) = \int_0^T \left(\int_0^l F(x)\phi(x, t)dx\right) \delta G(t)dt + \frac{1}{2}\int_0^T \left[r(0)\delta u_{xx}(0, t)\right]^2 dt.$$

3. This increment formula leads to an explicit gradient formula, is the above substiturion is justified.

4.5(c). The ITSP: Justification of the substiturion - A

$$\boxed{p(t) = r(0)u_{xx}(0,t) + \mathcal{M}(t), \;\; t \in [0,T]}$$

1. In practice the Neumann measured output $\mathcal{M}(t)$ belongs to $L^2(0,T)$.

4.5(c). The ITSP: Justification of the substiturion - A

$$\boxed{p(t) = r(0)u_{xx}(0,t) + \mathcal{M}(t), \;\; t \in [0,T]}$$

1. In practice the Neumann measured output $\mathcal{M}(t)$ belongs to $L^2(0,T)$.
2. Hence the condition $p \in L^2(0,T)$ in Lemma 4.3 is a natural one.

4.5(c). The ITSP: Justification of the substiturion - A

$$\boxed{p(t) = r(0)u_{xx}(0,t) + \mathcal{M}(t), \;\; t \in [0,T]}$$

1. In practice the Neumann measured output $\mathcal{M}(t)$ belongs to $L^2(0,T)$.
2. Hence the condition $p \in L^2(0,T)$ in Lemma 4.3 is a natural one.
3. On the other hand, the weak solution $\phi \in L^2(0,T;\mathcal{V}(0,l))$ of the adjoint problem exists under the regularity condition $p \in H^2(0,T)$,

4.5(c). The ITSP: Justification of the substiturion - A

$$\boxed{p(t) = r(0)u_{xx}(0,t) + \mathcal{M}(t), \;\; t \in [0,T]}$$

1. In practice the Neumann measured output $\mathcal{M}(t)$ belongs to $L^2(0,T)$.
2. Hence the condition $p \in L^2(0,T)$ in Lemma 4.3 is a natural one.
3. On the other hand, the weak solution $\phi \in L^2(0,T;\mathcal{V}(0,l))$ of the adjoint problem exists under the regularity condition $p \in H^2(0,T)$,
4. as Theorem 8 of [Alemdar Hasanov & Onur Baysal, *Inverse Problems* (2019)] and the solvability results given in [Onur Baysal & Alemdar Hasanov, *Appl. Math. Letters* (2019)] show.

4.5(c). The ITSP: Justification of the substiturion - A

$$\boxed{p(t) = r(0)u_{xx}(0,t) + \mathcal{M}(t), \;\; t \in [0,T]}$$

1. In practice the Neumann measured output $\mathcal{M}(t)$ belongs to $L^2(0,T)$.
2. Hence the condition $p \in L^2(0,T)$ in Lemma 4.3 is a natural one.
3. On the other hand, the weak solution $\phi \in L^2(0,T;\mathcal{V}(0,l))$ of the adjoint problem exists under the regularity condition $p \in H^2(0,T)$,
4. as Theorem 8 of [Alemdar Hasanov & Onur Baysal, *Inverse Problems* (2019)] and the solvability results given in [Onur Baysal & Alemdar Hasanov, *Appl. Math. Letters* (2019)] show.
5. This means that one needs to define a *weaker solution* of the adjoint problem.

4.5(c). The ITSP: Justification of the substiturion - A

$$\boxed{p(t) = r(0)u_{xx}(0,t) + \mathcal{M}(t), \ \ t \in [0,T]}$$

1. In practice the Neumann measured output $\mathcal{M}(t)$ belongs to $L^2(0,T)$.
2. Hence the condition $p \in L^2(0,T)$ in Lemma 4.3 is a natural one.
3. On the other hand, the weak solution $\phi \in L^2(0,T;\mathcal{V}(0,l))$ of the adjoint problem exists under the regularity condition $p \in H^2(0,T)$,
4. as Theorem 8 of [Alemdar Hasanov & Onur Baysal, *Inverse Problems* (2019)] and the solvability results given in [Onur Baysal & Alemdar Hasanov, *Appl. Math. Letters* (2019)] show.
5. This means that one needs to define a *weaker solution* of the adjoint problem.
6. Remark that similar situation arises in the Cauchy problem for elliptic equations [D.N. Hào, et. al, *Journal of Inverse and Ill-Posed Problems*, 26(2018)], where the `very weak solution` has first been introduced.

4.5(d). The ITSP: Justification of the substiturion - B

$$\boxed{p(t) = r(0)u_{xx}(0,t) + \mathcal{M}(t), \;\; t \in [0,T]}$$

1. Indeed, the increment formula provides further insight into this solution:
$\delta J(G) = \int_0^T \left(\int_0^l F(x)\phi(x,t)dx \right) \delta G(t)dt + \frac{1}{2}\int_0^T \left[r(0)\delta u_{xx}(0,t) \right]^2 dt.$

4.5(d). The ITSP: Justification of the substiturion - B

$$\boxed{p(t) = r(0)u_{xx}(0,t) + \mathcal{M}(t), \;\; t \in [0,T]}$$

1. Indeed, the increment formula provides further insight into this solution:
$\delta J(G) = \int_0^T \left(\int_0^l F(x)\phi(x,t)dx \right) \delta G(t)dt + \frac{1}{2} \int_0^T \left[r(0)\delta u_{xx}(0,t) \right]^2 dt.$
2. Namely, this formula suggest that for existence of the first right hand-side integral the condition $\phi \in L^2(0,T; L^2(0,l))$ is sufficient.

4.5(d). The ITSP: Justification of the substiturion - B

$$\boxed{p(t) = r(0)u_{xx}(0,t) + \mathcal{M}(t), \;\; t \in [0,T]}$$

1. Indeed, the increment formula provides further insight into this solution: $\delta J(G) = \int_0^T \left(\int_0^l F(x)\phi(x,t)dx \right) \delta G(t)dt + \frac{1}{2}\int_0^T \left[r(0)\delta u_{xx}(0,t)\right]^2 dt.$
2. Namely, this formula suggest that for existence of the first right hand-side integral the condition $\phi \in L^2(0,T;L^2(0,l))$ is sufficient.
3. This motivates the following definition.

4.5(d). The ITSP: Justification of the substiturion - B

$$\boxed{p(t) = r(0)u_{xx}(0,t) + \mathcal{M}(t), \;\; t \in [0,T]}$$

1. Indeed, the increment formula provides further insight into this solution: $\delta J(G) = \int_0^T \left(\int_0^l F(x)\phi(x,t)dx \right) \delta G(t)dt + \frac{1}{2}\int_0^T \left[r(0)\delta u_{xx}(0,t)\right]^2 dt.$
2. Namely, this formula suggest that for existence of the first right hand-side integral the condition $\phi \in L^2(0,T;L^2(0,l))$ is sufficient.
3. This motivates the following definition.
4. **Definition 4.1.** A function $\phi \in L^2(0,T;L^2(0,l))$ satisfying the integral identity

$$\int_0^T \int_0^l \phi(x,t)P(x,t)dxdt = \int_0^T r(0)v_{xx}(0,t)p(t)dt, \; \forall P \in \mathcal{P},$$

is defined a weaker solution of the adjoint problem, where $\mathcal{P}$ is a dense set in $L^2(0,T;L^2(0,l)$ and $v(x,t)$ is the weak solution of the following problem:

$$\begin{cases} \rho(x)v_{tt} + \mu(x)v_t + (r(x)v_{xx})_{xx} = P(x,t), \text{ in } \Omega_T, \\ v(x,0) = 0, \;\; v_t(x,0) = 0, \quad x \in (0,l), \\ v(0,t) = v_x(0,t) = 0, \;\; r(l)v_{xx}(l,t) = (r(l)v_{xx}(l,t))_x = 0, \;\; t \in [0,T]. \end{cases}$$

4.5(e). The ITSP: The Existence of the Fréchet Differential

1. It is clear that the above defined weaker solution is unique.

4.5(e). The ITSP: The Existence of the Fréchet Differential

1. It is clear that the above defined weaker solution is unique.
2. Indeed, if $\phi_1, \phi_2 \in \mathcal{P}$ two weaker solutions, then $\tilde{\phi} = \phi_1 - \phi_2$ solves the integral identity

$$\int_0^T \int_0^l \tilde{\phi}(x,t)P(x,t)dxdt = 0, \ \forall P \in \mathcal{P}.$$

4.5(e). The ITSP: The Existence of the Fréchet Differential

1. It is clear that the above defined weaker solution is unique.
2. Indeed, if $\phi_1, \phi_2 \in \mathcal{P}$ two weaker solutions, then $\tilde{\phi} = \phi_1 - \phi_2$ solves the integral identity
$$\int_0^T \int_0^l \tilde{\phi}(x,t) P(x,t) dxdt = 0, \ \forall P \in \mathcal{P}.$$
3. This implies that $\phi_1(x,t) = \phi_2(x,t)$, a.e. $(x,t) \in \Omega_T$, since $\mathcal{P}$ is dense in $L^2(0,T; L^2(0,l))$.

4.5(e). The ITSP: The Existence of the Fréchet Differential

1. It is clear that the above defined weaker solution is unique.
2. Indeed, if $\phi_1, \phi_2 \in \mathcal{P}$ two weaker solutions, then $\tilde{\phi} = \phi_1 - \phi_2$ solves the integral identity

$$\int_0^T \int_0^l \tilde{\phi}(x,t)P(x,t)dxdt = 0, \ \forall P \in \mathcal{P}.$$

3. This implies that $\phi_1(x,t) = \phi_2(x,t)$, a.e. $(x,t) \in \Omega_T$, since $\mathcal{P}$ is dense in $L^2(0,T;L^2(0,l))$.
4. **Theorem 4.2.** Let the main conditions hold and $G \in \mathbf{G}$. Assume that $\phi \in L^2(0,T;L^2(0,l))$ is the weaker solution of the adjoint problem. Then the Tikhonov functional is Fréchet differentiable. Moreover, for the Fréchet gradient of this functional the following explicit gradient formula holds:

$$\boxed{J'(G)(t) = \int_0^l F(x)\phi(x,t)dx, \ \text{a.e. } t \in (0,T)}$$

4.5(e). The ITSP: The Existence of the Fréchet Differential

1. It is clear that the above defined weaker solution is unique.
2. Indeed, if $\phi_1, \phi_2 \in \mathcal{P}$ two weaker solutions, then $\tilde{\phi} = \phi_1 - \phi_2$ solves the integral identity
$$\int_0^T \int_0^l \tilde{\phi}(x,t)P(x,t)dxdt = 0, \ \forall P \in \mathcal{P}.$$
3. This implies that $\phi_1(x,t) = \phi_2(x,t)$, a.e. $(x,t) \in \Omega_T$, since $\mathcal{P}$ is dense in $L^2(0,T;L^2(0,l))$.
4. **Theorem 4.2.** Let the main conditions hold and $G \in \mathbf{G}$. Assume that $\phi \in L^2(0,T;L^2(0,l))$ is the weaker solution of the adjoint problem. Then the Tikhonov functional is Fréchet differentiable. Moreover, for the Fréchet gradient of this functional the following explicit gradient formula holds:
$$\boxed{J'(G)(t) = \int_0^l F(x)\phi(x,t)dx, \ \text{a.e. } t \in (0,T)}$$
5. **Remark 4.1.** The similar gradient formula can be derived in the same way for the inverse problem of identifying the spatial load $F(x)$ from the Neumann measured boundary output, if $G(t)$ is assumed to be known.

4.6. The ITSP: Lipschitz continuity of the Fréchet gradient

1. The Lipschitz continuity of the Fréchet differential of the Tikhonov functional is an important property since it implies the monotonicity of the iterations $\{J(g^{(n)})\}$ of a gradient algorithm [A. Hasanov Hasanoglu and V.G. Romanov, *Introduction to Inverse Problems for Differential Equations*, New York: Springer (2017)].

4.6. The ITSP: Lipschitz continuity of the Fréchet gradient

1. The Lipschitz continuity of the Fréchet differential of the Tikhonov functional is an important property since it implies the monotonicity of the iterations $\{J(g^{(n)})\}$ of a gradient algorithm [A. Hasanov Hasanoglu and V.G. Romanov, *Introduction to Inverse Problems for Differential Equations*, New York: Springer (2017)].
2. However, it requires a smoother input.

4.6. The ITSP: Lipschitz continuity of the Fréchet gradient

1. The Lipschitz continuity of the Fréchet differential of the Tikhonov functional is an important property since it implies the monotonicity of the iterations $\{J(g^{(n)})\}$ of a gradient algorithm [A. Hasanov Hasanoglu and V.G. Romanov, *Introduction to Inverse Problems for Differential Equations*, New York: Springer (2017)].
2. However, it requires a smoother input.
3. **Theorem 4.3.** Let the main conditions hold and $G \in \mathbf{G}^3 \subset H^3(0,T)$. Assume, in addition, that the input satisfy also the following regularity conditions: $\rho \in H^4(0,l),\ \ r, F \in H^2(0,l)$.

4.6. The ITSP: Lipschitz continuity of the Fréchet gradient

1. The Lipschitz continuity of the Fréchet differential of the Tikhonov functional is an important property since it implies the monotonicity of the iterations $\{J(g^{(n)})\}$ of a gradient algorithm [A. Hasanov Hasanoglu and V.G. Romanov, *Introduction to Inverse Problems for Differential Equations*, New York: Springer (2017].
2. However, it requires a smoother input.
3. **Theorem 4.3.** Let the main conditions hold and $G \in \mathbf{G}^3 \subset H^3(0,T)$. Assume, in addition, that the input satisfy also the following regularity conditions: $\rho \in H^4(0,l),\ r, F \in H^2(0,l)$.
4. Then the Fréchet gradient of the Tikhonov functional is Lipschitz continuous, that is

$$\|J'(G_1) - J'(G_2)\|_{L^2(0,T)} \le L_G \, \|G_1 - G_2\|_{H^3(0,T)}, \ \forall G_1, G_2 \in \mathbf{G}^3,\ L_G(T) > 0.$$

4.7(a1). The ITSP: The Reconstruction Algorithm (Basics-1)

The reconstruction procedure is based on minimizing the Tikhonov functional by using the following Conjugate Gradient Algorithm (CGA).

1. **Step 1:** Input the initial iteration $G^{(0)}(t) \equiv 0$ and find decent direction $p^{(0)} \equiv -J'(G^{(0)})$.

4.7(a1). The ITSP: The Reconstruction Algorithm (Basics-1)

The reconstruction procedure is based on minimizing the Tikhonov functional by using the following Conjugate Gradient Algorithm (CGA).

1. **Step 1:** Input the initial iteration $G^{(0)}(t) \equiv 0$ and find decent direction $p^{(0)} \equiv -J'(G^{(0)})$.
2. **Step 2:** Find the parameter

$$\alpha_*^{(i)} = \frac{||J'(G^{(i)})||^2_{L^2(0,T)}}{||-r(0)u_{xx}(0,\cdot;p^{(i)})||^2_{L^2(0,T)}}$$

from the minimization problem $J(G^{(i)}(t) + \alpha_*^{(i)} p^{(i)}(t)) = \min_{\alpha>0} J(G^{(i)}(t) + \alpha p^{(i)}(t))$;
then define the next iteration $G^{(i+1)}(t) = G^{(i)}(t) + \alpha_*^{(i)} p^{(i)}(t)$ and compute $J(G^{(i+1)})$.

4.7(a1). The ITSP: The Reconstruction Algorithm (Basics-1)

The reconstruction procedure is based on minimizing the Tikhonov functional by using the following Conjugate Gradient Algorithm (CGA).

1. **Step 1:** Input the initial iteration $G^{(0)}(t) \equiv 0$ and find decent direction $p^{(0)} \equiv -J'(G^{(0)})$.
2. **Step 2:** Find the parameter

$$\alpha_*^{(i)} = \frac{||J'(G^{(i)})||^2_{L^2(0,T)}}{||-r(0)u_{xx}(0,\cdot;p^{(i)})||^2_{L^2(0,T)}}$$

   from the minimization problem $J(G^{(i)}(t) + \alpha_*^{(i)} p^{(i)}(t)) = \min_{\alpha>0} J(G^{(i)}(t) + \alpha p^{(i)}(t))$; then define the next iteration $G^{(i+1)}(t) = G^{(i)}(t) + \alpha_*^{(i)} p^{(i)}(t)$ and compute $J(G^{(i+1)})$.
3. **Step 3:** Set $i = i + 1$, compute $J'_h(G^{(i)})$ and the descent direction $p^{(i)}(t)$ by the formula:

$$p^{(i)}(t) = \frac{\|J'(G^{(i)})\|^2_{L^2(0,T)}}{\|J'(G^{(i-1)})\|^2_{L^2(0,T)}}\, p^{(i-1)}(t) - J'(G^{(i)})(t).$$

4.7(a1). The ITSP: The Reconstruction Algorithm (Basics-1)

The reconstruction procedure is based on minimizing the Tikhonov functional by using the following Conjugate Gradient Algorithm (CGA).

1. **Step 1:** Input the initial iteration $G^{(0)}(t) \equiv 0$ and find decent direction $p^{(0)} \equiv -J'(G^{(0)})$.
2. **Step 2:** Find the parameter

$$\alpha_*^{(i)} = \frac{||J'(G^{(i)})||^2_{L^2(0,T)}}{||-r(0)u_{xx}(0,\cdot;p^{(i)})||^2_{L^2(0,T)}}$$

from the minimization problem $J(G^{(i)}(t) + \alpha_*^{(i)} p^{(i)}(t)) = \min_{\alpha>0} J(G^{(i)}(t) + \alpha p^{(i)}(t))$; then define the next iteration $G^{(i+1)}(t) = G^{(i)}(t) + \alpha_*^{(i)} p^{(i)}(t)$ and compute $J(G^{(i+1)})$.
3. **Step 3:** Set $i = i + 1$, compute $J_h'(G^{(i)})$ and the descent direction $p^{(i)}(t)$ by the formula:

$$p^{(i)}(t) = \frac{\|J'(G^{(i)})\|^2_{L^2(0,T)}}{\|J'(G^{(i-1)})\|^2_{L^2(0,T)}}\, p^{(i-1)}(t) - J'(G^{(i)})(t).$$

4. **Step 4:** If the stopping condition below holds, for known parameter $\tau_M > 1$, stop the iteration process; otherwise, return to Step 2.

4.7(a1). The ITSP: The Reconstruction Algorithm (Basics-2)

1. Morozov's Discrepancy Principle is used as the stopping condition

$$\begin{aligned} &\|[-r(0)u_{xx}(0,\cdot;G^{(i)})] - \mathcal{M}^{\gamma}\|_{L^2(0,T)} \leq \tau_M \delta \\ &\qquad < \|[-r(0)u_{xx}(0,\cdot;G^{(i-1)})] - \mathcal{M}^{\gamma}\|_{L^2(0,T)}, \ \tau_M > 1. \end{aligned}$$

4.7(a1). The ITSP: The Reconstruction Algorithm (Basics-2)

1. Morozov's Discrepancy Principle is used as the stopping condition

$$
\begin{aligned}
||[-r(0)u_{xx}(0,\cdot;G^{(i)})] - \mathcal{M}^{\gamma}||_{L^2(0,T)} &\leq \tau_M \delta \\
&< ||[-r(0)u_{xx}(0,\cdot;G^{(i-1)})] - \mathcal{M}^{\gamma}||_{L^2(0,T)}, \ \ \tau_M > 1.
\end{aligned}
$$

2. The method of lines approach is employed. That is, on the spatial domain weak problem is discretized by Finite Element Method with Hermite cubic basis functions while time discretization is done by second order implicit finite difference scheme to obtain full discrete problem.

4.7(a1). The ITSP: The Reconstruction Algorithm (Basics-2)

1. Morozov's Discrepancy Principle is used as the stopping condition

$$
\begin{aligned}
&\|[-r(0)u_{xx}(0,\cdot;G^{(i)})]-\mathcal{M}^{\gamma}\|_{L^2(0,T)} \le \tau_M\delta \\
&\qquad < \|[-r(0)u_{xx}(0,\cdot;G^{(i-1)})]-\mathcal{M}^{\gamma}\|_{L^2(0,T)}, \ \tau_M > 1.
\end{aligned}
$$

2. The method of lines approach is employed. That is, on the spatial domain weak problem is discretized by Finite Element Method with Hermite cubic basis functions while time discretization is done by second order implicit finite difference scheme to obtain full discrete problem.
3. In detail, both the direct and adjoint problems are solved efficiently on an appropriate Finite Element mesh with Hermite cubic basis functions.

4.7(a1). The ITSP: The Reconstruction Algorithm (Basics-2)

1. Morozov's Discrepancy Principle is used as the stopping condition

$$
\begin{aligned}
&||[-r(0)u_{xx}(0,\cdot;G^{(i)})] - \mathcal{M}^{\gamma}||_{L^2(0,T)} \le \tau_M \delta \\
&\qquad < ||[-r(0)u_{xx}(0,\cdot;G^{(i-1)})] - \mathcal{M}^{\gamma}||_{L^2(0,T)}, \ \tau_M > 1.
\end{aligned}
$$

2. The method of lines approach is employed. That is, on the spatial domain weak problem is discretized by Finite Element Method with Hermite cubic basis functions while time discretization is done by second order implicit finite difference scheme to obtain full discrete problem.
3. In detail, both the direct and adjoint problems are solved efficiently on an appropriate Finite Element mesh with Hermite cubic basis functions.
4. While time discretization is done by second order implicit finite difference scheme to obtain full discrete problem.

4.7(a2). The ITSP: The Reconstruction Algorithm (Details)

1. The noise free synthetic output data $\mathcal{M}_h(t_j) := [-r(x)u_{hxx}(x, t_j; G)]_{x=0}$ is obtained from the numerical solution of the direct problem. Then the random noisy data $\mathcal{M}_h^{\gamma}(t_j) := \mathcal{M}_h(t_j) + \gamma \, \|\mathcal{M}_h\|_{L^2(0,T)}\mathrm{randn}(N)$, with the noise level $\gamma \geq 0$ is produced by using the MATLAB `randn` function.

4.7(a2). The ITSP: The Reconstruction Algorithm (Details)

1. The noise free synthetic output data $\mathcal{M}_h(t_j) := [-r(x)u_{h_{xx}}(x,t_j;G)]_{x=0}$ is obtained from the numerical solution of the direct problem. Then the random noisy data $\mathcal{M}_h^{\gamma}(t_j) := \mathcal{M}_h(t_j) + \gamma \, \|\mathcal{M}_h\|_{L^2(0,T)}\mathrm{randn}(N)$, with the noise level $\gamma \geq 0$ is produced by using the MATLAB `randn` function.
2. To study the convergence and accuracy of the algorithm the behavior of the convergence error $e(i;G;\gamma) = \| \left[-r(x)u_{h_{xx}}(x,\cdot;G^{(i)})\right]_{x=0} - \mathcal{M}_h^{\delta}\|_{L^2(0,T)}$ and the accuracy error $E(i;G;\gamma) = \|G - G^{(i)}\|_{L^2(0,T)}$ are analyzed on the test problems.

4.7(a2). The ITSP: The Reconstruction Algorithm (Details)

1. The noise free synthetic output data $\mathcal{M}_h(t_j) := [-r(x)u_{h_{xx}}(x, t_j; G)]_{x=0}$ is obtained from the numerical solution of the direct problem. Then the random noisy data $\mathcal{M}_h^{\gamma}(t_j) := \mathcal{M}_h(t_j) + \gamma \, \|\mathcal{M}_h\|_{L^2(0,T)}\mathrm{randn}(N)$, with the noise level $\gamma \geq 0$ is produced by using the MATLAB `randn` function.
2. To study the convergence and accuracy of the algorithm the behavior of the convergence error $e(i; G; \gamma) = \| \left[-r(x)u_{h_{xx}}(x, \cdot; G^{(i)})\right]_{x=0} - \mathcal{M}_h^{\delta}\|_{L^2(0,T)}$ and the accuracy error $E(i; G; \gamma) = \|G - G^{(i)}\|_{L^2(0,T)}$ are analyzed on the test problems.
3. The CGA is implemented in the examples below with and without regularization. *In all numerical examples below the CGA without regularization achieves better accuracy. The reason, as was established first in [Nemirovskii, 1986] and then proved in [Hanke, 1995], is that the CGA is itself a regularization algorithm.*

4.7(a2). The ITSP: The Reconstruction Algorithm (Details)

1. The noise free synthetic output data $\mathcal{M}_h(t_j) := [-r(x)u_{h_{xx}}(x, t_j; G)]_{x=0}$ is obtained from the numerical solution of the direct problem. Then the random noisy data $\mathcal{M}_h^\gamma(t_j) := \mathcal{M}_h(t_j) + \gamma\,\|\mathcal{M}_h\|_{L^2(0,T)}\mathrm{randn}(N)$, with the noise level $\gamma \geq 0$ is produced by using the MATLAB `randn` function.
2. To study the convergence and accuracy of the algorithm the behavior of the convergence error $e(i; G; \gamma) = \| \left[-r(x)u_{h_{xx}}(x, \cdot; G^{(i)})\right]_{x=0} - \mathcal{M}_h^\delta\|_{L^2(0,T)}$ and the accuracy error $E(i; G; \gamma) = \|G - G^{(i)}\|_{L^2(0,T)}$ are analyzed on the test problems.
3. The CGA is implemented in the examples below with and without regularization. *In all numerical examples below the CGA without regularization achieves better accuracy. The reason, as was established first in [Nemirovskii, 1986] and then proved in [Hanke, 1995], is that the CGA is itself a regularization algorithm.*
4. Speed of the algorithm can be seen as reasonable for basic computer configuration (i5 Intel processor with 4gb 1333MHz Ram). Actually CPU time is about 3 sec. per 10 iterations, but it can be accelerated with minor changes in algorithm or on improved computer configurations.

4.8(b1). The ITSP: Numerical Results (types of temporal loads)

1. The performance of the proposed algorithm is illustrated by 3 different benchmark test problems.

4.8(b1). The ITSP: Numerical Results (types of temporal loads)

1. The performance of the proposed algorithm is illustrated by 3 different benchmark test problems.
2. The following three types of temporal $G(t)$ and spatial $F(x)$ loads given in Table 1 are we employed in the numerical simulations to illustrate the performance of the CGA.

4.8(b1). The ITSP: Numerical Results (types of temporal loads)

1. The performance of the proposed algorithm is illustrated by 3 different benchmark test problems.
2. The following three types of temporal $G(t)$ and spatial $F(x)$ loads given in Table 1 are we employed in the numerical simulations to illustrate the performance of the CGA.
3. **Table 1.** Temporal and spatial loads employed in the numerical experiments

	Test 1	**Test 2**	**Test 3**
$F(x)$	x	e^x	$\delta_{0.9}^{\epsilon}(x)$
$G(t)$	$t\sin(4\pi t)$	$\kappa(1/2-t)+\kappa(t-1/2)\sin(3\pi t)$	$t(1-t)^2$

4.8(b1). The ITSP: Numerical Results (types of temporal loads)

1. The performance of the proposed algorithm is illustrated by 3 different benchmark test problems.
2. The following three types of temporal $G(t)$ and spatial $F(x)$ loads given in Table 1 are we employed in the numerical simulations to illustrate the performance of the CGA.
   3. **Table 1.** Temporal and spatial loads employed in the numerical experiments

	Test 1	**Test 2**	**Test 3**
$F(x)$	x	e^x	$\delta^{\epsilon}_{0.9}(x)$
$G(t)$	$t\sin(4\pi t)$	$\kappa(1/2-t)+\kappa(t-1/2)\sin(3\pi t)$	$t(1-t)^2$

4. where $\kappa(t)$ is the Heaviside step function.

4.8(b2). The ITSP: Numerical Results (Reconstruction of a Smooth Temporal Load)

1. The first test problem: an oscillating smooth temporal load: $G(t) = t\sin(4\pi t)$ $(F(x) = x)$

4.8(b2). The ITSP: Numerical Results (Reconstruction of a Smooth Temporal Load)

1. The first test problem: an oscillating smooth temporal load: $G(t) = t\sin(4\pi t)$ $(F(x) = x)$
2. The results with the noise levels $\gamma \in \{0, 0.03, 0.05\}$ in $\mathcal{M}_h^\gamma$

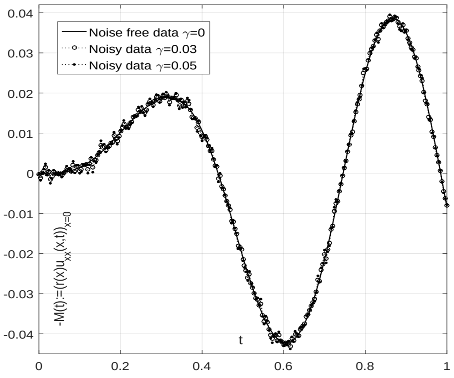

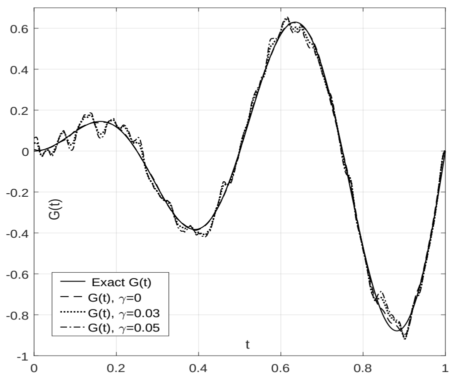

Figure: Synthetic noise free and noisy outputs (left), the reconstructed temporal load (right)

4.8(b3). The ITSP: Numerical Results (Convergence and Accuracy Errors)

1. The convergence error $e(i; G; \gamma) = \| \left[-r(x)u_{h_{xx}}(x, \cdot; G^{(i)})\right]_{x=0} - \mathcal{M}_h^{\delta}\|_{L^2(0,T)}$ and the accuracy error $E(i; G; \gamma) = \|G - G^{(i)}\|_{L^2(0,T)}$

4.8(b3). The ITSP: Numerical Results (Convergence and Accuracy Errors)

1. The convergence error $e(i;G;\gamma) = \| \left[-r(x) u_{h_{xx}}(x,\cdot;G^{(i)}) \right]_{x=0} - \mathcal{M}_h^\delta \|_{L^2(0,T)}$ and the accuracy error $E(i;G;\gamma) = \| G - G^{(i)} \|_{L^2(0,T)}$
2.

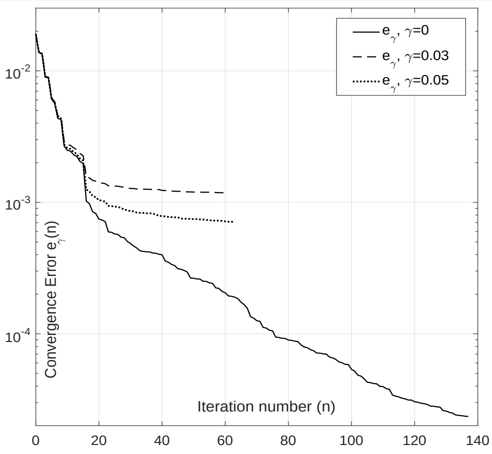

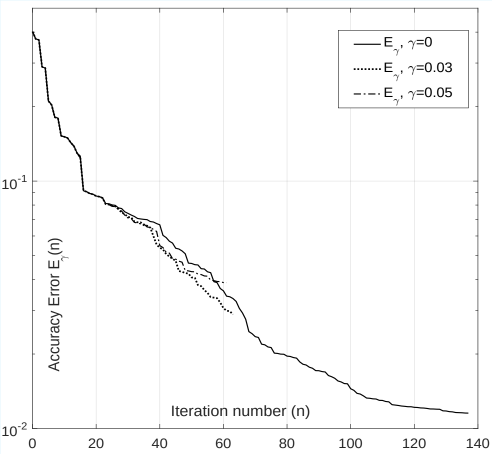

4.8(b4). The ITSP: Numerical Results (Reconstruction of a Non-Smooth Temporal Load)

1. The second test problem: a non-smooth temporal load: $G(t) = \kappa(1/2 - t) + \kappa(t - 1/2)\sin(3\pi t)$ $(F(x) = \exp(x))$

4.8(b4). The ITSP: Numerical Results (Reconstruction of a Non-Smooth Temporal Load)

1. The second test problem: a non-smooth temporal load:
   $G(t) = \kappa(1/2 - t) + \kappa(t - 1/2)\sin(3\pi t)$ $(F(x) = \exp(x))$
2. The results with the noise levels $\gamma \in \{0, 0.03, 0.05\}$ in $\mathcal{M}_h^\gamma$

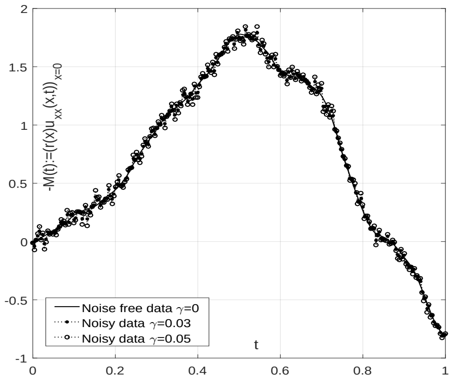

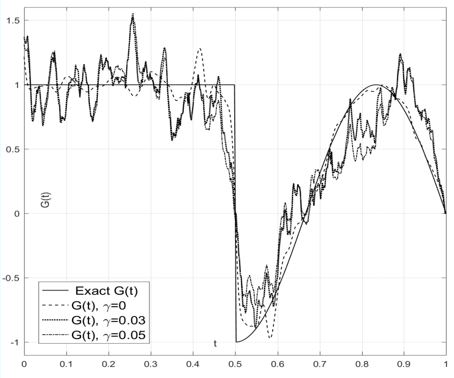

Figure: Synthetic noise free and noisy outputs (left), the reconstructed temporal load (right)

4.8(b4). The ITSP: Numerical Results (Pointwise Spatial Load)

1. The third test problem: The spatial load $F(x) = \delta^{\epsilon}_{0.9}(x)$, where $\delta^{\epsilon}_{x_0} = \exp(-(x - x_0)^2/\epsilon)/\sqrt{\pi\epsilon}$ with small $\epsilon > 0$ is the approximation of Dirac delta.

4.8(b4). The ITSP: Numerical Results (Pointwise Spatial Load)

1. The third test problem: The spatial load $F(x) = \delta^{\epsilon}_{0.9}(x)$, where $\delta^{\epsilon}_{x_0} = \exp(-(x-x_0)^2/\epsilon)/\sqrt{\pi\epsilon}$ with small $\epsilon > 0$ is the approximation of Dirac delta.
2. The results with the noise levels $\gamma \in \{0, 0.03, 0.05\}$

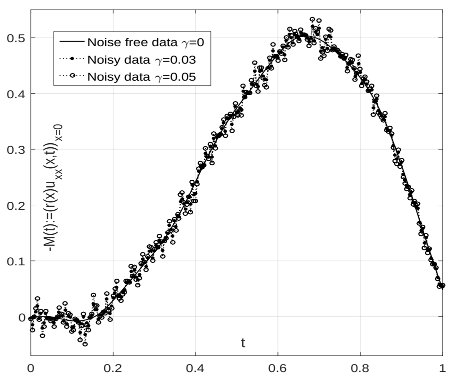

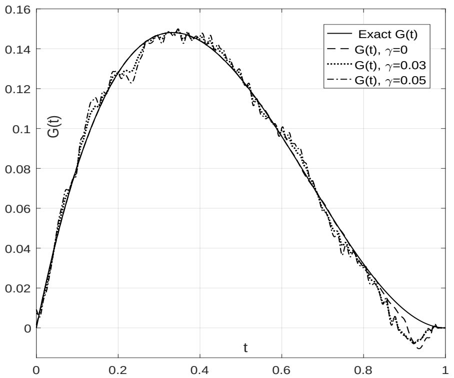

Figure: Synthetic noise free and noisy outputs (left), the reconstructed temporal load (right)

5. Some Conclusions

1. The theory given here covers all existing basic physical models.

5. Some Conclusions

1. The theory given here covers all existing basic physical models.
2. This theory is applicable to all basic (”clamped”, ”supported” and ”free”) boundary conditions.

5. Some Conclusions

1. The theory given here covers all existing basic physical models.
2. This theory is applicable to all basic ("clamped", "supported" and "free") boundary conditions.
3. It requires minimal smoothness from the inputs and outputs.

5. Some Conclusions

1. The theory given here covers all existing basic physical models.
2. This theory is applicable to all basic ("clamped", "supported" and "free") boundary conditions.
3. It requires minimal smoothness from the inputs and outputs.
4. This theory allows to construct effective and fast numerical algorithms.

Unsolved Inverse Problems for the Dynamic Euler-Bernoulli Beam

1. Uniqueness of a solution to the Inverse Temporal Source Problem.

Unsolved Inverse Problems for the Dynamic Euler-Bernoulli Beam

1. Uniqueness of a solution to the Inverse Temporal Source Problem.
2. Uniqueness of a solution to the Inverse Boundary Value Problem for a cantilever beam with the Neumann boundary measured output.

Unsolved Inverse Problems for the Dynamic Euler-Bernoulli Beam

1. Uniqueness of a solution to the Inverse Temporal Source Problem.
2. Uniqueness of a solution to the Inverse Boundary Value Problem for a cantilever beam with the Neumann boundary measured output.
3. Inverse coefficient problems based on boundary measured outputs.

Unsolved Inverse Problems for the Dynamic Euler-Bernoulli Beam

1. Uniqueness of a solution to the Inverse Temporal Source Problem.
2. Uniqueness of a solution to the Inverse Boundary Value Problem for a cantilever beam with the Neumann boundary measured output.
3. Inverse coefficient problems based on boundary measured outputs.
4. **Remark.** A uniqueness results for the solution of the inverse boundary value problem for a cantilever beam, in the case of the Neumann-to-Dirichlet operator, is proved in [Alemdar Hasanov, Onur Baysal and Cristiana Sebu, Identification of an unknown shear force in the Euler-Bernoulli cantilever beam from measured boundary deflection, *Inverse Problems*, 2019].

Some References - 1

1. A. Hasanov, Identification of an unknown source term in a vibrating cantilevered beam from final overdetermination, *Inverse Problems* **25** (2009) 115015 (19pp).

Some References - 1

1. A. Hasanov, Identification of an unknown source term in a vibrating cantilevered beam from final overdetermination, *Inverse Problems* **25** (2009) 115015 (19pp).
2. A. Hasanov and O. Baysal, Identification of an unknown spatial load distribution in a vibrating cantilevered beam from final overdetermination, *Journal of Inverse and Ill-Posed Problems* **23** (1)(2015) 85-102.

Some References - 1

1. A. Hasanov, Identification of an unknown source term in a vibrating cantilevered beam from final overdetermination, *Inverse Problems* **25** (2009) 115015 (19pp).
2. A. Hasanov and O. Baysal, Identification of an unknown spatial load distribution in a vibrating cantilevered beam from final overdetermination, *Journal of Inverse and Ill-Posed Problems* **23** (1)(2015) 85-102.
3. A. Hasanov and O. Baysal, Identification of unknown temporal and spatial load distributions in a vibrating Euler-Bernoulli beam from Dirichlet boundary measured data, *Automatica*, **71** (2016), 106-117

Some References - 1

1. A. Hasanov, Identification of an unknown source term in a vibrating cantilevered beam from final overdetermination, *Inverse Problems* **25** (2009) 115015 (19pp).
2. A. Hasanov and O. Baysal, Identification of an unknown spatial load distribution in a vibrating cantilevered beam from final overdetermination, *Journal of Inverse and Ill-Posed Problems* **23** (1)(2015) 85-102.
3. A. Hasanov and O. Baysal, Identification of unknown temporal and spatial load distributions in a vibrating Euler-Bernoulli beam from Dirichlet boundary measured data, *Automatica*, **71** (2016), 106-117
4. A. Hasanov and A. Kawano, Identification of unknown spatial load distributions in a vibrating Euler-Bernoulli beam from limited measured data *Inverse Problems*, **32** (2016) 055004 (16pp)

Some References - 1

1. A. Hasanov, Identification of an unknown source term in a vibrating cantilevered beam from final overdetermination, *Inverse Problems* **25** (2009) 115015 (19pp).
2. A. Hasanov and O. Baysal, Identification of an unknown spatial load distribution in a vibrating cantilevered beam from final overdetermination, *Journal of Inverse and Ill-Posed Problems* **23** (1)(2015) 85-102.
3. A. Hasanov and O. Baysal, Identification of unknown temporal and spatial load distributions in a vibrating Euler-Bernoulli beam from Dirichlet boundary measured data, *Automatica*, **71** (2016), 106-117
4. A. Hasanov and A. Kawano, Identification of unknown spatial load distributions in a vibrating Euler-Bernoulli beam from limited measured data *Inverse Problems*, **32** (2016) 055004 (16pp)
5. A. Hasanov and Hiromichi Itou, A priori estimates for the general form dynamic Euler-Bernoulli beam equation: supported and cantilever beams, *Applied Mathematics Letters*, **87** (2019) 141-146.

Some References - 2

1. O. Baysal and A. Hasanov, Solvability of initial and boundary value problem for clamped Euler-Bernoulli beam, *Applied Mathematics Letters*, **93** (2019) 85-90.

Some References - 2

1. O. Baysal and A. Hasanov, Solvability of initial and boundary value problem for clamped Euler-Bernoulli beam, *Applied Mathematics Letters*, **93** (2019) 85-90.
2. A. Hasanov, O. Baysal and C. Sebu, Identification of an unknown shear force in the Euler-Bernoulli cantilever beam from measured boundary deflection, *Inverse Problems* (2019). DOI: 10.1088/1361-6420/ab2a34.

Some References - 2

1. O. Baysal and A. Hasanov, Solvability of initial and boundary value problem for clamped Euler-Bernoulli beam, *Applied Mathematics Letters*, **93** (2019) 85-90.
2. A. Hasanov, O. Baysal and C. Sebu, Identification of an unknown shear force in the Euler-Bernoulli cantilever beam from measured boundary deflection, *Inverse Problems* (2019). DOI: 10.1088/1361-6420/ab2a34.
3. A. Hasanov and O. Baysal, Identification of a temporal in a cantilever beam from measured boundary bending moment, *Inverse Problems* (2019). DOI: 10.1088/1361-6420/ab2aa9.

1. I would like to take this opportunity to thank Professor Roman Novikov once again for the warm welcome and hospitality he showed to me during my first official visit to this university.

I would like to take this opportunity to thank Professor Roman Novikov once again for the warm welcome and hospitality he showed to me during my first official visit to this university.

1. I would like to take this opportunity to thank Professor Roman Novikov once again for the warm welcome and hospitality he showed to me during my first official visit to this university.
2. Thank You For Your Attention.